NOAA Technical Report NESDIS 56

A NOISE LEVEL ANALYSIS OF SPECIAL 10-SPIN-PER-CHANNEL VAS DATA

Washington, D.C.
February 1991

U.S. DEPARTMENT OF COMMERCE
National Oceanic and Atmospheric Administration
National Environmental Satellite, Data, and Information Service

NOAA TECHNICAL REPORTS

National Environmental Satellite, Data, and Information Service

...mental Satellite, Data, and Information Service (NESDIS) manages the Nation's civil Earth-observing ... as global national data bases for meteorology, oceanography, geophysics, and solar-terrestrial sciences. From these sources, it develops and disseminates environmental data and information products critical to the protection of life and property, national defense, the national economy, energy development and distribution, global food supplies, and the development of natural resources.

Publication in the NOAA Technical Report series does not preclude later publication in scientific journals in expanded or modified form. The NESDIS series of NOAA Technical Reports is a continuation of the former NESS and EDIS series of NOAA Technical Reports and the NESC and EDS series of Environmental Science Services Administration (ESSA) Technical Reports.

A limited number of copies are available by contacting Nancy Everson, NOAA/NESDIS, E/RA22, 5200 Auth Road, Washington, DC, 20233. Copies can also be ordered from the National Technical Information Service (NTIS), U.S. Department of Commerce, Sills Bldg., 5285 Port Royal Road, Springfield, VA. 22161, (703) 487-4650 (prices on request for paper copies or microfiche, please refer to PB number when ordering). A partial listing of more recent reports appear below:

NESDIS 5 A Statistical Technique for Forecasting Severe Weather from Vertical Soundings by Satellite and Radiosonde. David L. Keller and William L. Smith, June 1983. (PB84 114099)

NESDIS 6 Spatial and Temporal Distribution of Northern Hemisphere Snow Cover. Burt J. Morse and Chester F. Ropelewski (NWS), October 1983. (PB84 118348)

NESDIS 7 Fire Detection Using the NOAA--Series Satellites. Michael Matson, Stanley R. Schneider, Billie Aldridge and Barry Satchwell (NWS), January 1984. (PB84 176890)

NESDIS 8 Monitoring of Long Waves in the Eastern Equatorial Pacific 1981-83 Using Satellite Multi-Channel Sea Surface Temperature Charts. Richard Legeckis and William Pichel, April 1984. (PB84 190487)

NESDIS 9 The NESDIS-SEL Lear Aircraft Instruments and Data Recording System. Gilbert R. Smith, Kenneth O. Hayes, John S. Knoll and Robert S. Koyanagi, June 1984. (PB84 219674)

NESDIS 10 Atlas of Reflectance Patterns for Uniform Earth and Cloud Surfaces (NIMBUS-7 ERB--61 Days). V.R. Taylor and L.L. Stowe, July 1984. (PB85 12440)

NESDIS 11 Tropical Cyclone Intensity Analysis Using Satellite Data. Vernon F. Dvorak, September 1984. (PB85 112951)

NESDIS 12 Utilization of the Polar Platform of NASA's Space Station Program for Operational Earth Observations. John H. McElroy and Stanley R. Schneider, September 1984. (PB85 1525027AS)

NESDIS 13 Summary and Analyses of the NOAA N-ROSS/ERS-1 Environmental Data Development Activity. John W. Sherman III, February 1984. (PB85 222743/43)

NESDIS 14 NOAA N-ROSS/ERS-1 Environmental Data Development (NNEEDD) Activity. John W. Sherman III, February 1985. (PB86 139284 A/S)

NESDIS 15 NOAA N-ROSS/ERS-1 Environmental Data Development (NNEEDD) Products and Services. Franklin E. Kniskern, February 1985, (PB86 213527/AS)

NESDIS 16 Temporal and Spatial Analyses of Civil Marine Satellite Requirements. Nancy J. Hooper and John W. Sherman III, February 1985. (PB86 212123/AS)

NESDIS 18 Earth Observations and the Polar Platform. John H. McElroy and Stanley R. Schneider, January 1985. (PB85 177624/AS)

NESDIS 19 The Space Station Polar Platform: Intergrating Research and Operational Missions. John H. McElroy and Stanley R. Schneider, January 1985. (PB85 195279/AS)

NESDIS 20 An Atlas of High Altitude Aircraft Measured Radiance of White Sands, New Mexico, in the 450-1050nm Band. Gilbert R. Smith, Robert H. Levin and John S. Knoll, April 1985. (PB85 204501/AS)

NESDIS 21 High Altitude Measured Radiance of White Sands, New Mexico, in the 400-2000nm Band Using a Filter Wedge Spectrometer. Gilbert R. Smith and Robert H. Levin, April 1985. (PB85 206084/AS)

NESDIS 22 The Space Station Polar Platform: NOAA Systems Considerations and Requirements. John H. McElroy and Stanley R. Schneider, June 1985. (PB86 6109246/AS)

NOAA Technical Report NESDIS 56

A NOISE LEVEL ANALYSIS OF SPECIAL 10-SPIN-PER-CHANNEL VAS DATA

Donald W. Hillger
James F.W. Purdom
Regional and Mesoscale Meteorology Branch (RAMM)

and

Debra A. Lubich
Cooperative Institute for Research in the Atmosphere (CIRA)

Colorado State University
Fort Collins, CO 80523-0033

Washington, D.C.
February 1991

U.S. DEPARTMENT OF COMMERCE
Robert A. Mosbacher, Secretary

National Oceanic and Atmospheric Administration
John A. Knauss, Under Secretary

National Environmental Satellite, Data, and Information Service
Thomas N. Pyke, Jr. , Assistant Administrator

CONTENTS

LIST OF FIGURES

Page

LIST OF TABLES

Page

A NOISE LEVEL ANALYSIS OF SPECIAL 10-SPIN-PER-CHANNEL VAS DATA

Donald W. Hillger
James F.W. Purdom

NESDIS, Regional and Mesoscale Meteorology (RAMM) Branch

Debra A. Lubich

Cooperative Institute for Research in the Atmosphere (CIRA)

Colorado State University (CSU)
Fort Collins, CO 80523-0033

ABSTRACT

A special collection period for VAS (VISSR Atmospheric Sounder) data was arranged in order to test the effect of spin budget (multiple samples at the same FOV) on the noise levels of the VAS channels. This study employs three methods to determine the noise level of the VAS channel measurements and compares those measurements to the design specifications for the VAS instrument. Results from the three analysis methods agreed in general, but each method failed in certain situations. This indicates that no one method of determining noise levels is totally reliable for operational data sets.

Knowledge of noise levels is an important part of the use of any data set. Requirements for sounding accuracy can then be used to specify the spin budget (number of temporal samples) or the spatial averaging needed to meet those requirements. Although GOES-Next will not use multiple samples of the same FOVs to decrease noise levels, the dwell time may be increased to decrease noise levels. The change in noise level with dwell time should be tested with 'operational' data from GOES-Next.

1.0 INTRODUCTION

The spin budget for operational VAS data collection is from one to four spins for any given scan line of data depending on the channel. The additional spins for the various channels are averaged at each field-of-view (FOV) along a scan line to provide VAS radiances with lower noise levels than would be obtained from a single sample (1 spin) at each FOV. Spatial averaging of multiple FOVs is then used in operational situations to further reduce noise levels before producing thermodynamic soundings (Hayden, 1988). However spatial averaging was not considered in this study. Only the reduction in noise level due to multiple measurements at single FOVs was analyzed.

High-resolution VISSR Atmospheric Sounder (VAS) radiances with a spin budget of ten spins per channel were taken during a special data collection period in December 1989. The purpose of this special collection was to provide a data set for determining the optimal number of spins for each channel for producing single-FOV VAS thermodynamic soundings. The optimal number of spins is a tradeoff between the maximum number of spins which provide the lowest noise, while at the same time minimizing the number of spins so that a channel is not oversampled. Because of time constraints on satellite operation, oversampling reduces the total area that can be covered. By determining the noise level as a function of the number of spins for each channel, the number of spins can be determined where the noise level does not significantly decrease with additional spins. This is the optimal number of spins for that channel. Additional spins may slightly decrease noise levels but at the sacrifice of time needed to provide necessary spatial coverage.

Noise levels for this special VAS data were determined using three methods. The three methods were: 1) structure function analysis of measurements at adjacent FOVs; 2) variability of multiple measurements (samples) at each FOV; and 3) variability of space-view measurements.

Structure function analysis is a proven technique that allows the determination of noise levels using routine, but cloud-free data. A computer-intensive statistical analysis of the data is used to determine the structure function of the data, which is a combination of the spatial gradient and the noise within the data. By removing the spatial gradient from the structure, the remaining structure is equivalent to the relative noise determined from calibration measurements of several satellite instruments (Hillger and Vonder Haar, 1988).

The statistical variability of multiple measurements at each FOV can also be used to determine the noise level of the data. Since the individual samples from multiple spins are not saved in operational data sets, this method is only possible from special data collections which save the individual measurements at each FOV.

Finally, space-view measurements were analyzed for their noise level. The variability of these no-signal (off the Earth) measurements should be equal to the noise level of the instrument. Such space-view measurements are used to regularly determine the noise levels of operational data. Space-view results presented in this study were obtained from Dr. W. P. Menzel of NESDIS/CIMSS (Cooperative Institute for Meteorological Satellite Studies).

Plots of signal and noise levels versus the number of spins for each VAS channel will be shown. Structure function derived values will be compared with the statistical variability of multiple measurements at each FOV and with space-view noise level estimates. Additionally, a few selected retrievals will be shown to illustrate the effect of the number of spins on the variability of the retrieved temperature or dew point temperature profiles.

2.0 SPECIAL VAS DATA

A special VAS collection period in December 1989 was arranged through Dr. W. P. Menzel at NESDIS/CIMSS. During this period a limited area was scanned with each channel sampled ten times. Data were collected by the CIRA ground station for analysis. Table 1 provides some basic information about the VAS channels. This table can be used for reference regarding VAS channel characteristics.

Table 1

VAS Channel Information

VAS Channel	Filter Center (μm)	Effective Wavenumber (cm^{-1})	Approximate Peak Weight Level (hPa)	Best Horizontal Resolution (km)	FOV Size
1	14.7	680	70	16	large
2	14.5	690	125	16	large
3	14.3	700	200	8	small
4	14.0	715	500	8	small
5	13.3	750	920	8	small
6	4.5	2208	850	16	large
7	12.7	789	1000	8	small
8	11.2	897	surface	8	small
9	7.3	1375	600	8	small
10	6.8	1486	400	8	small
11	4.4	2253	300	16	large
12	3.9	2541	surface	16	large

Data were available only for a total of 10 different scan lines that covered the entire width of a full-disk image. Only the middle third of each scan line was saved to reduce computer storage and to eliminate measurements taken at large scan (zenith) angles. Of the middle third only a small area of 100 along-line FOVs (from each of the 10 scan lines) was chosen for intensive analysis. Data for all VAS channels were taken at their maximum horizontal resolution as shown in column 5 of Table 1. Figures 1a and 1b show the FOV locations for the small resolution (8 km at nadir) sensors and the large resolution (16 km at nadir) sensors, respectively. For large FOV sensors only 7 scan lines of data were available. (Note that only the line-to-line spacing changes between the small FOV and the large FOV sensors.) For both FOV sizes, the along-line spacing is equal (8 km at nadir).

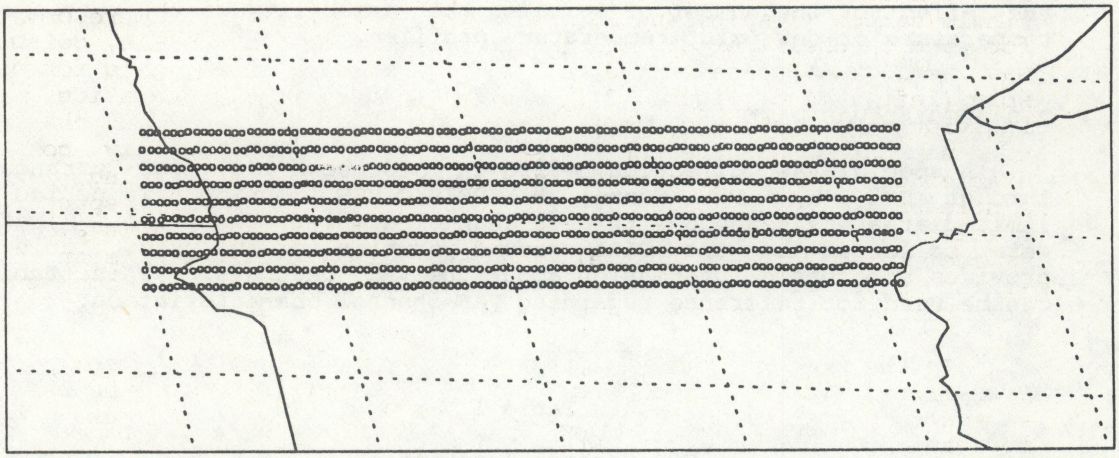

Figure 1a: Area of intensive analysis showing FOV locations for small resolution (8 km at nadir) VAS sensors. Each small circle represents the center point of one FOV.

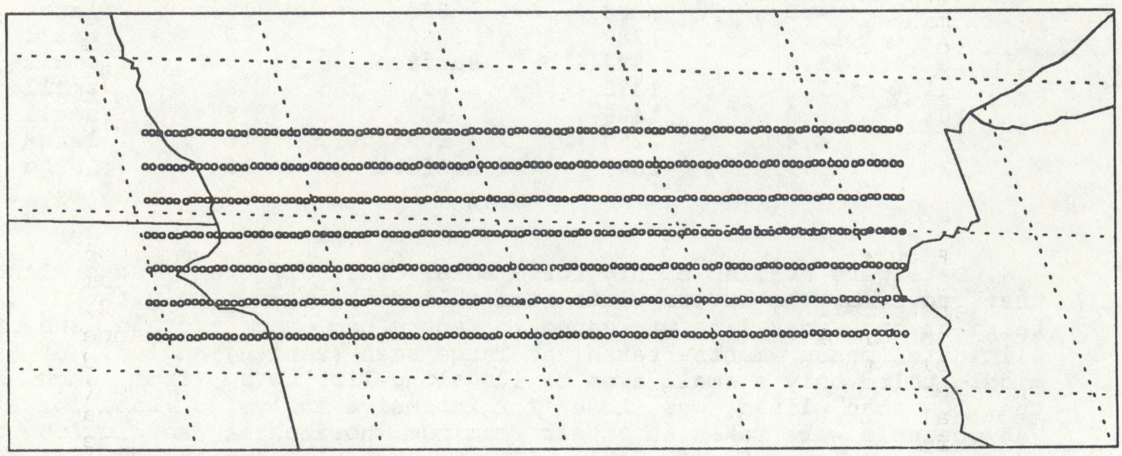

Figure 1b: Same as Figure 1a, but for large resolution (16 km at nadir) VAS sensors.

2.1 Data file organization

Figure 2 presents a schematic of the VAS data flow for this special data set. VAS data were organized into two different file structures in order to compute the necessary statistics. Twenty single-sample (1-spin) and 20 spin-averaged 'image' files were created for each channel. After first being saved in one large file, software was used to separate the data stream into an 'image' file for each spin (left side of Figure 2). Note that besides separation into individual spins, the small FOV channels and the large FOV channels were separated. The reason for this was to simultaneously compute statistics on VAS channels with equal line-to-line spacing. These single-sample data files were used to compute the repeat-view statistics. Additional software was used to produce spin-averaged 'image' files for each channel with from 1 to 10 spins per scan line (right side of Figure 2). These data files were used to compute the structure-estimated noise levels.

In the original data stream the various channels and spins are transmitted in a mixed (non-consecutive) order. At the time of separation into data files for each spin, the VAS data were reorganized into a form where scan lines are consecutive. With consecutive scan lines a file can be displayed as an image, thus the term 'image' files used above. Conversion from measured count values to effective blackbody temperatures and navigation of the data takes place at the time of separation into 'image' files.

3.0 STRUCTURE ANALYSIS

One method of determining the noise level of satellite measurements is by structure function analysis on a subset of the data (Hillger and Vonder Haar, 1979, and 1988; Wald, 1989) Structure analysis statistically compares measurements at adjacent FOVs to determine the gradient as a function of separation distance (Gomis and Alonso, 1988). The structure function is then extrapolated to zero separation distance, effectively taking the spatial gradient out of the statistics. The remaining structure can be shown to be twice the noise variance (the square of the standard error [σ]) (Gandin, 1963),

$$\text{structure at zero separation distance} = 2\sigma^2 . \quad (1)$$

Figures 3a and 3b show typical structure analyses with polynomials fitted to the discrete structure values. Four polynomials are shown in each figure, least-squares fitted to the first 2, 3, 4, and 5 discrete structure values. In Figure 3a, for VAS channel 5, all the polynomials have nearly identical intercepts at zero distance. However in Figure 3b, for VAS channel 7 with a steeper slope (stronger spatial gradient), the intercepts are different. In such a case, the best-fit zero distance value is based on a minimum in the unexplained variance between the polynomial and the discrete structure values. Consistency among the polynomials fitted to different numbers of structure values is also important. This is done to detect and eliminate polynomials fitted to individual structure values which may be unrepresentative of the true structure at small distances. The best-fit zero distance values were then used to compute the standard errors using the inverse of Equation 1.

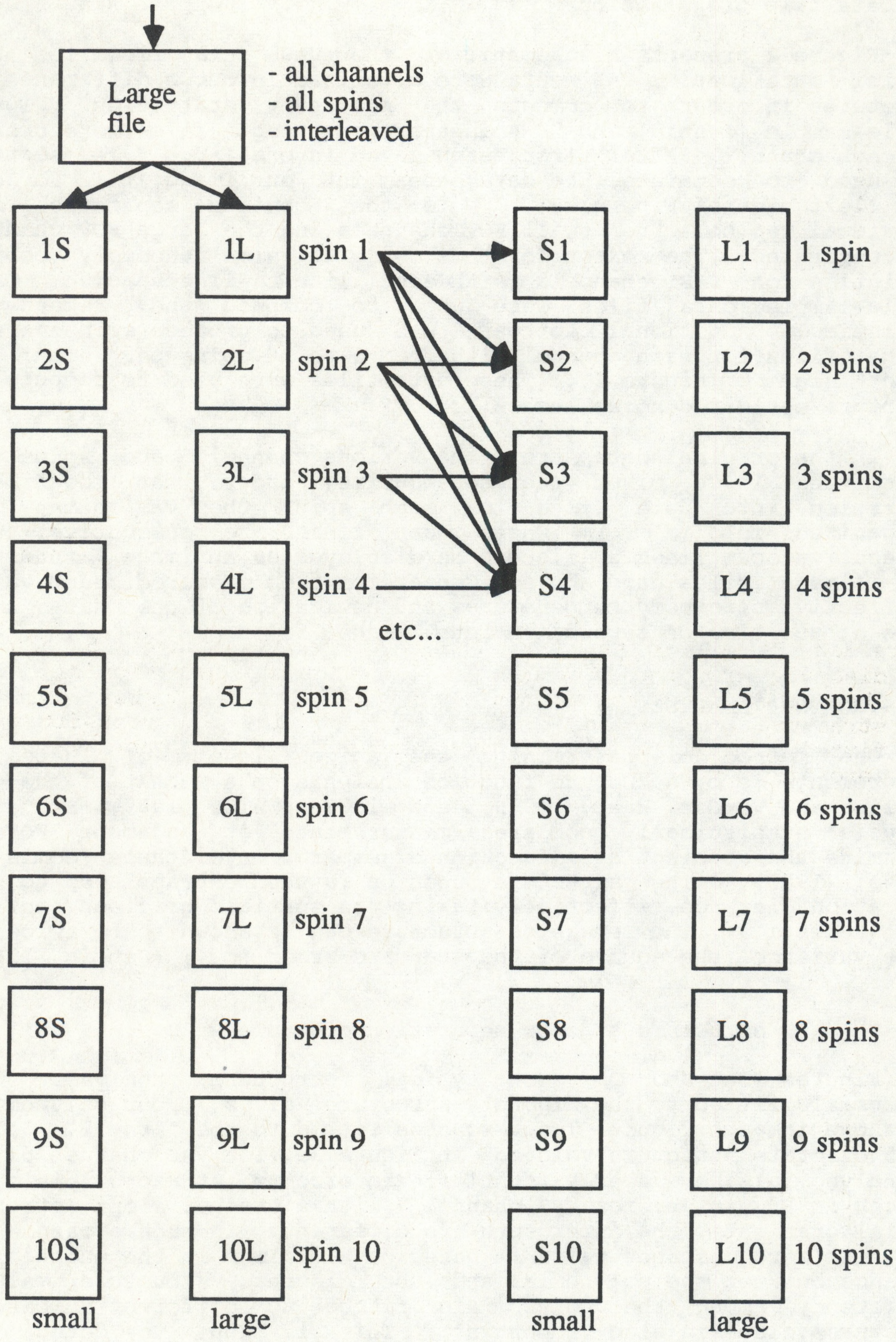

S = Small sensors (VAS channels 3,4,5,7,8,9,10)
L = Large sensors (VAS channels 1,2,6,11,12)
- de-interleaved, calibrated, navigated

Figure 2: Ten-spin data flow for special VAS data collection.

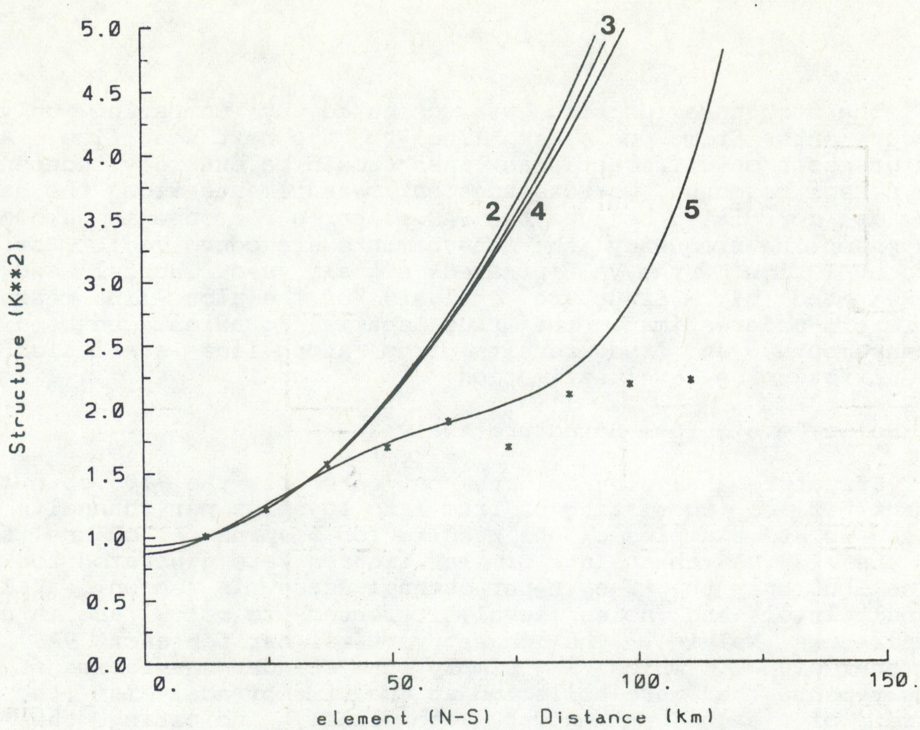

Figure 3a: Example of structure analysis for VAS channel 5 showing discrete structure values as a function of separation distance. The number next to each polynomials is the number discrete structure values in the least-squares fit. The best-fit among fitted polynomials is used to determine the structure value at zero distance.

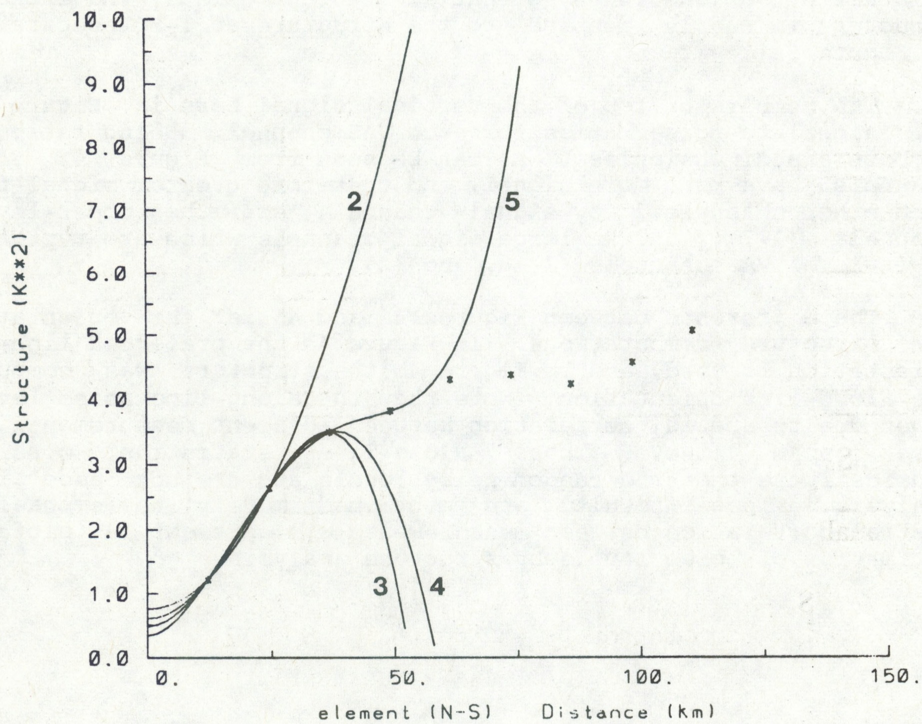

Figure 3b: Same as Figure 3a, but for VAS channel 7.

The structure function was computed by comparing only those measurements from one scan line to the next scan line. Adjacent measurements on different scan lines should be entirely independent of any sensor response, whereas adjacent measurements along the same scan line are correlated because the VAS sensor's response is slower than its sampling frequency (the measurements are convolved). For details on convolution of the VAS infrared signal, see Gabriel and Purdom (1990a and b). Structure analysis of the along-line measurements therefore underestimates the true spatial gradient between nearby measurements, and the results from along-line statistics are not useful for noise level estimation.

3.1 Noise Levels from Structure Analysis

Structure analysis was run on each of the 10 spin-averaged 'image' files consisting of from 1 to 10 spins per channel. Figures 4a and 4b are examples of the results for 5 spins per channel for each of the 12 VAS channels. Similar figures were generated for 1 to 10 spins, but only the 5-spin-per-channel case is shown. Values of signal level and noise level, referred to below, are in units of temperature (kelvin). The longest vertical bar for each VAS channel is the signal, which is simply the standard deviation of all the measurements that were collected at the time of analysis (the middle third of each full-width scan line), indicating the natural variability of the weather seen in the VAS channels. Two estimates of the noise level are given. The longer of the two shorter vertical bars is the noise level from the structure at 1-FOV separation. This non-zero distance value may contain spatial gradient information and therefore overestimate the actual noise level. The shortest vertical bar is the noise level from the estimated structure at zero separation distance. In some situations the extrapolation resulted in lower noise levels when spatial gradient was present at 1-FOV separation. In other situations (when no spatial gradient exists) the extrapolated structure in nearly identical to the structure at 1-FOV separation (as in Figure 3a).

The numbers on top of the vertical signal bars in Figure 4 are the signal-to-noise ratios for each VAS channel. Being ratios, these numbers are dimensionless. As can be seen from Figure 4, some VAS channels have much more signal, and therefore greater signal-to-noise than other channels. Low signal channels are the upper-level VAS channels (1-3), unlike large signal channels which are typically the lower-level VAS channels (7, 8, and 12).

The difference between Figures 4a and 4b is the orientation of the structure computations. In Figure 4a the preferred line-to-line orientation is used, and in Figure 4b the structure was computed in the along-line orientation. Note that the along-line noise levels are lower due to spatial correlation between adjacent measurements on the same scan line. These along-line statistics consistently underestimate the true random noise levels and are not used in this analysis. These results are mentioned merely to emphasize that spatial correlation between measurements can present a pitfall for estimation of noise levels by structure analysis.

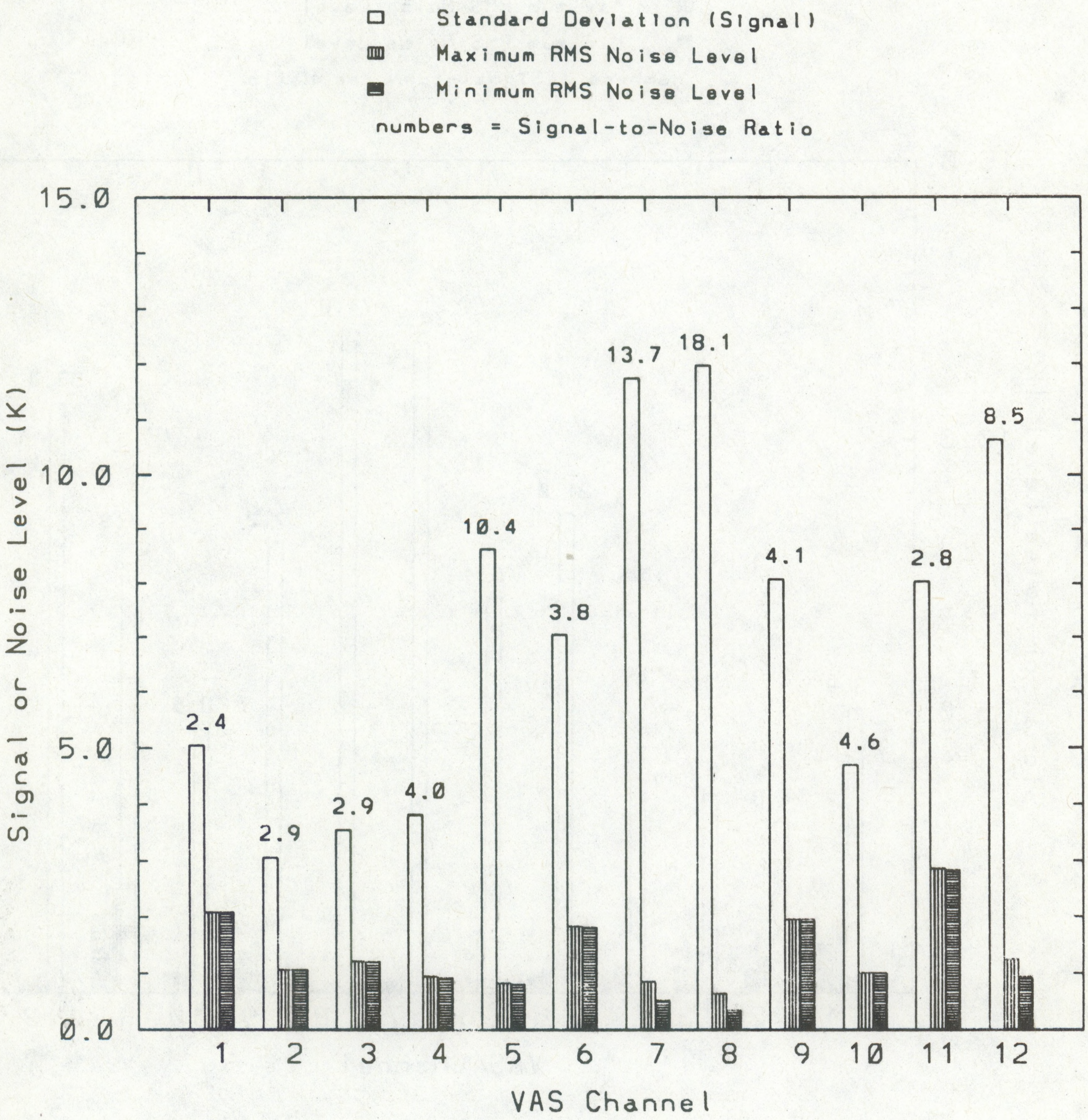

Figure 4a: Example of noise level analysis for 5 spins per channel for each of the 12 VAS channels. For each VAS channel the longest vertical bar is signal, the two shorter vertical bars (see legend) are maximum and minimum noise level estimates. Numbers on top of the vertical signal bars are dimensionless signal-to-noise ratios. Statistics are computed in the preferred line-to-line orientation to avoid along-line correlations due to sensor response.

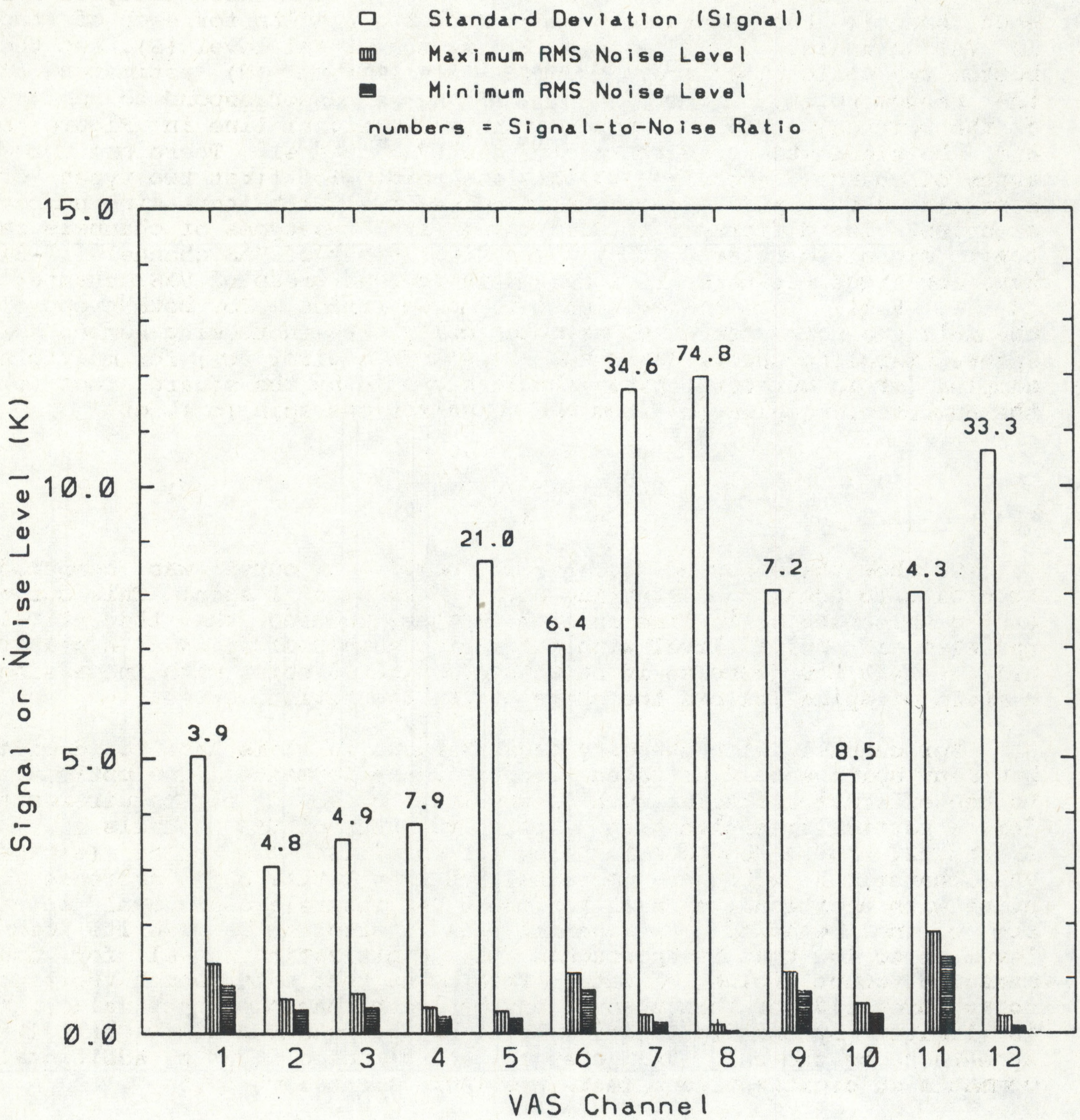

Figure 4b: Same as Figure 4a but using statistics computed in the along-line orientation. Measurements in this orientation are correlated due to sensor response, and noise levels are reduced due to smearing of spatial gradient information compared to measurements in the line-to-line orientation.

3.2 Noise Level as a Function of the Number of Spins

To determine the effect of the number of spins on noise level, the spin-averaged measurements for 1 to 10 spins were analyzed for each channel. Figures 5a through 5l show the results for each of the 12 VAS channels. The top solid line is the signal level (S), and the bottom two solid lines are maximum (X) and minimum (N) estimates of the random noise, described above. These lines correspond to numbers on the vertical axis. The numbers above the signal line in Figure 5 are the signal-to-noise ratios for each VAS channel. There are three types of channels according to this analysis. The first two types of channels show a strong decrease in noise level with increasing number of spins. The difference between those first two types of channels is their signal-to-noise ratio. The first group of VAS channels (1-3) have low signal-to-noise ratios, and the second group of VAS channels (4, 6, 9-11) have higher signal-to-noise ratios. For both types of channels the noise decreases asymptotically with increasing number of spins. Sampling theory says that the standard error (σ_n) for multiple samples (or in our case spins) should decrease by the square root of the number of samples (n) from the noise for one spin (σ_1), or

$$\sigma_n = \sigma_1 / n^{1/2} . \qquad (2)$$

To show the expected decrease in noise, a curve was computed according to Equation 2 starting with the value at 1 spin. This curve is the unlabeled solid line on each graph, showing the theoretical decrease in noise level with increasing number of spins. In nearly all channels the decrease in structure-estimated noise with increasing numbers of spins follows the shape of the theoretical curve.

For channels with steadily decreasing noise it is hard to decide how many spins should be taken to optimize performance. One option is to use external criteria, such as absolute noise level requirements for a particular application. The third group of VAS channels (5, 7, 8, and 12) show a decrease in noise for the first few spins (except VAS channel 8 with no decrease) and then little or no decrease in noise with additional spins. For these VAS channels additional spins are of no benefit. VAS channel 8 is interesting because its noise level is so low that it approaches the digitization level for one measured count value of data. This means that even though the true noise threshold for this channel may be lower than one count value, it is limited by the digitization level of the measurements. Channel 8 appears to be the only VAS channel so affected. Some additional comments on digitization effects are included in Section 5.

3.3 Implications of Noise Analysis

Noise level results such as those shown above can be used to determine future spin budgets for VAS. Table 2 compares the spin budget presently used, column 2, to two estimates of the number of spins required based on noise analysis presented above. Column 3 presents the spin budget when the noise levels do not decrease significantly for additional spins. This would be a minimum number of spins to reach a significantly lower noise level, a very qualitative determination. The numbers in columns 2 and 3 either agree or their ranges overlap, the exception being VAS channel 12 where only one spin is taken and two or more spins are needed. The last column in Table 2

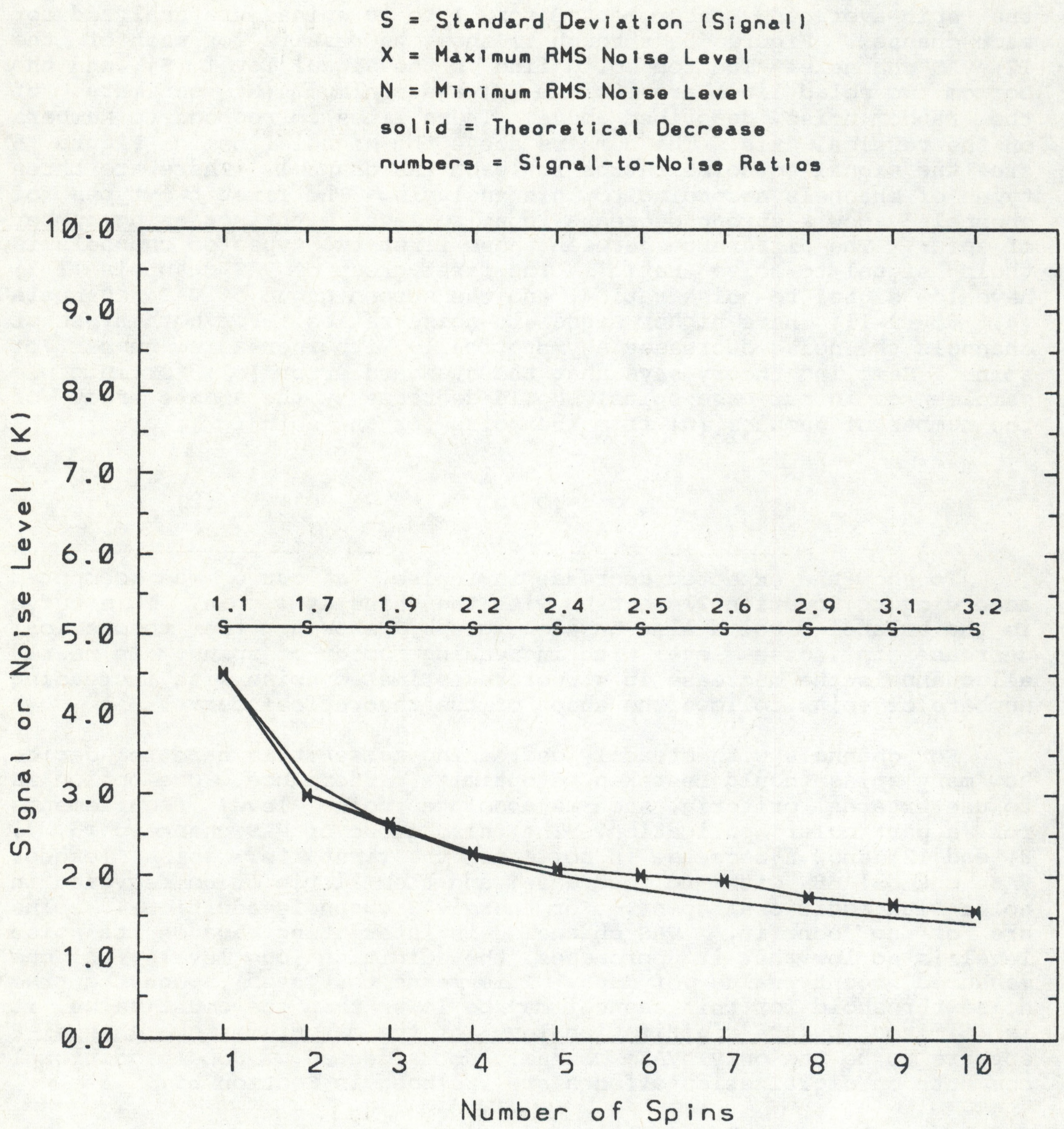

Figure 5a: Structure-estimated noise level as a function of the number of spins for VAS channel 1. Labeling of lines (S, X, and N) is explained in the text and in the legend on top. The unlabeled solid line is the theoretical decrease in noise level with increasing number of spins (samples). All solid lines correspond to the numbers on the vertical axis. The numbers above the signal line are the signal-to-noise ratios for each VAS channel. Measurements from adjacent FOVs are statistically compared in the line-to-line orientation.

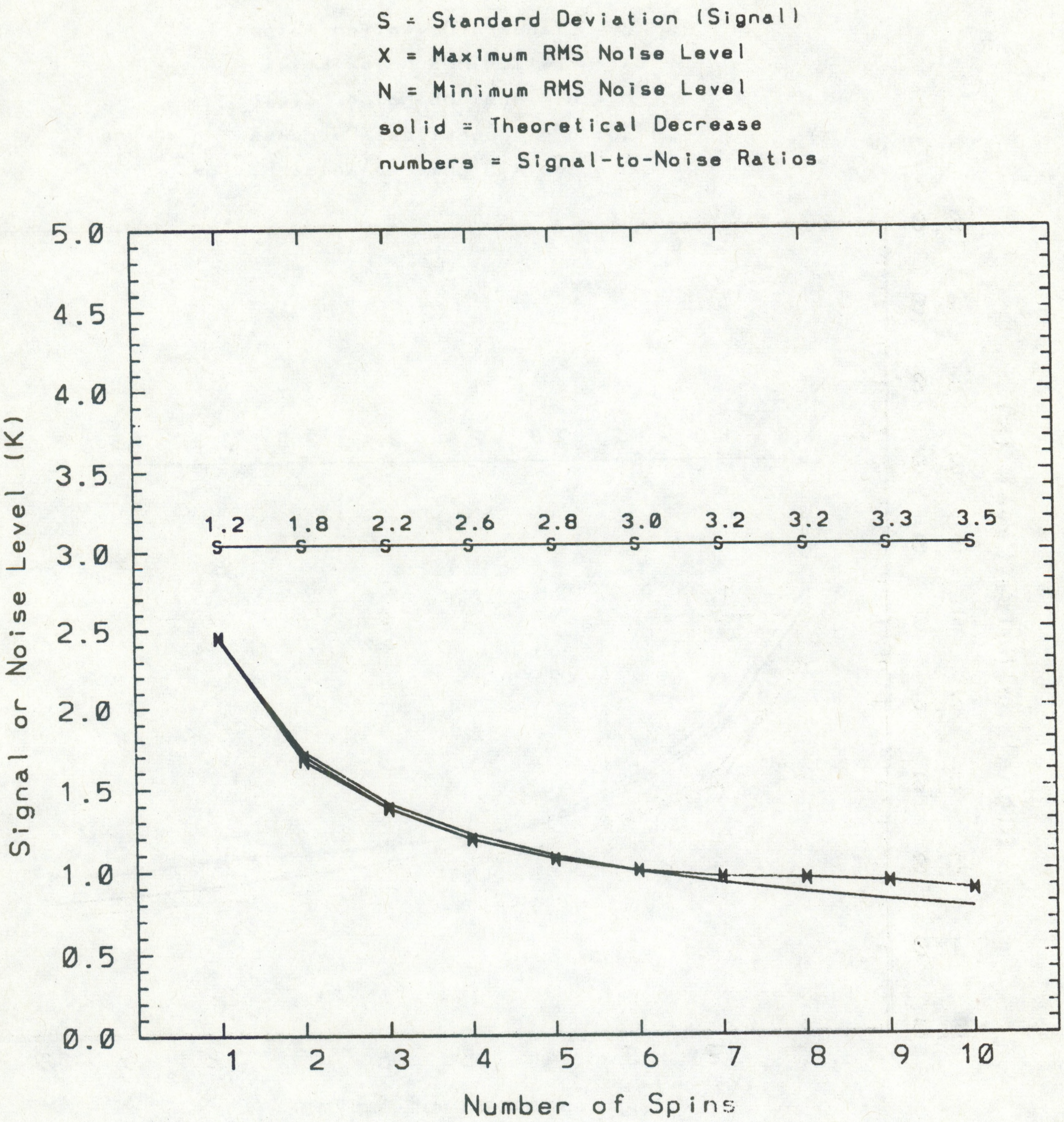

Figure 5b: Same as Figure 5a, but for VAS channel 2.

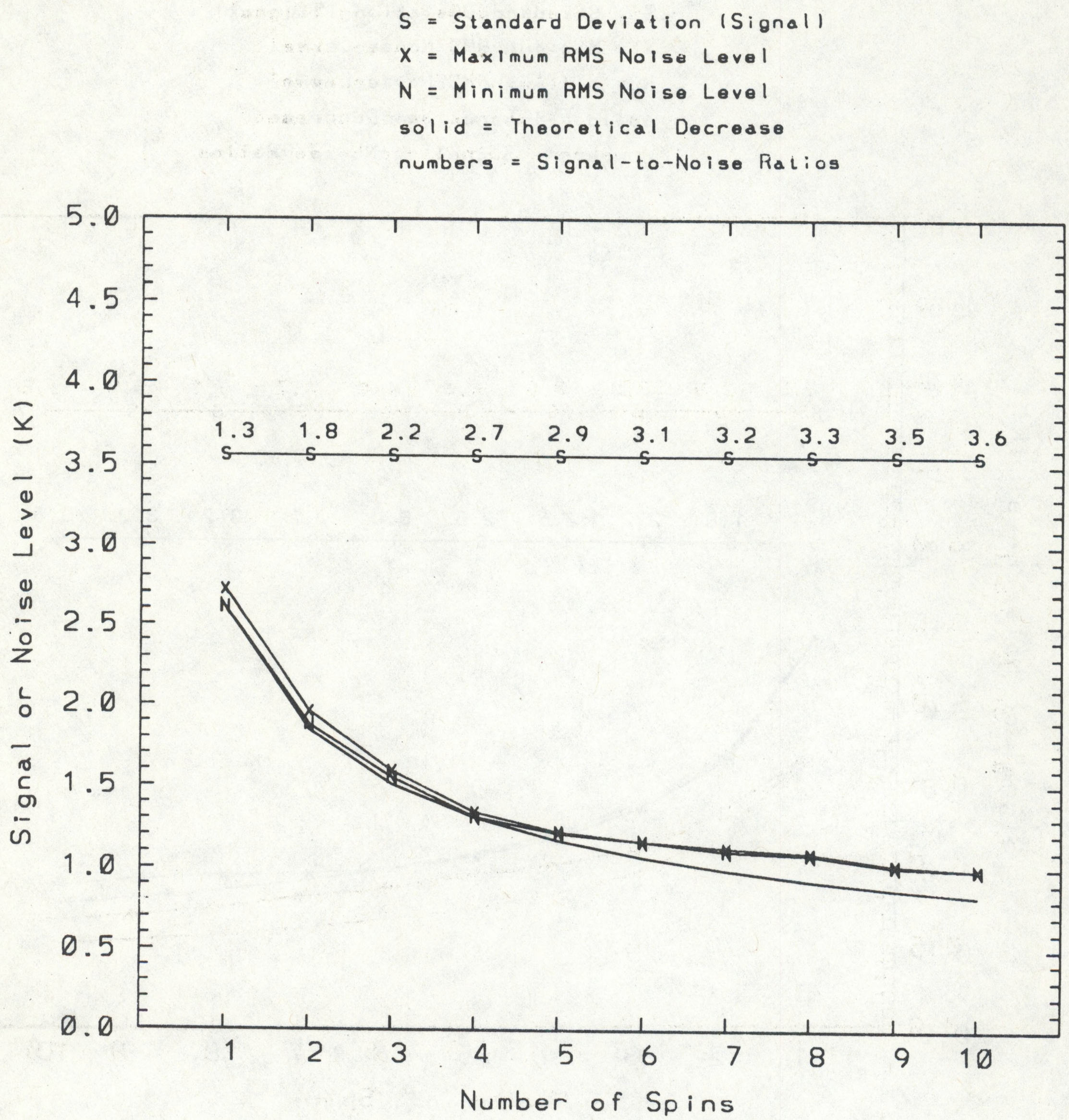

Figure 5c: Same as Figure 5a, but for VAS channel 3.

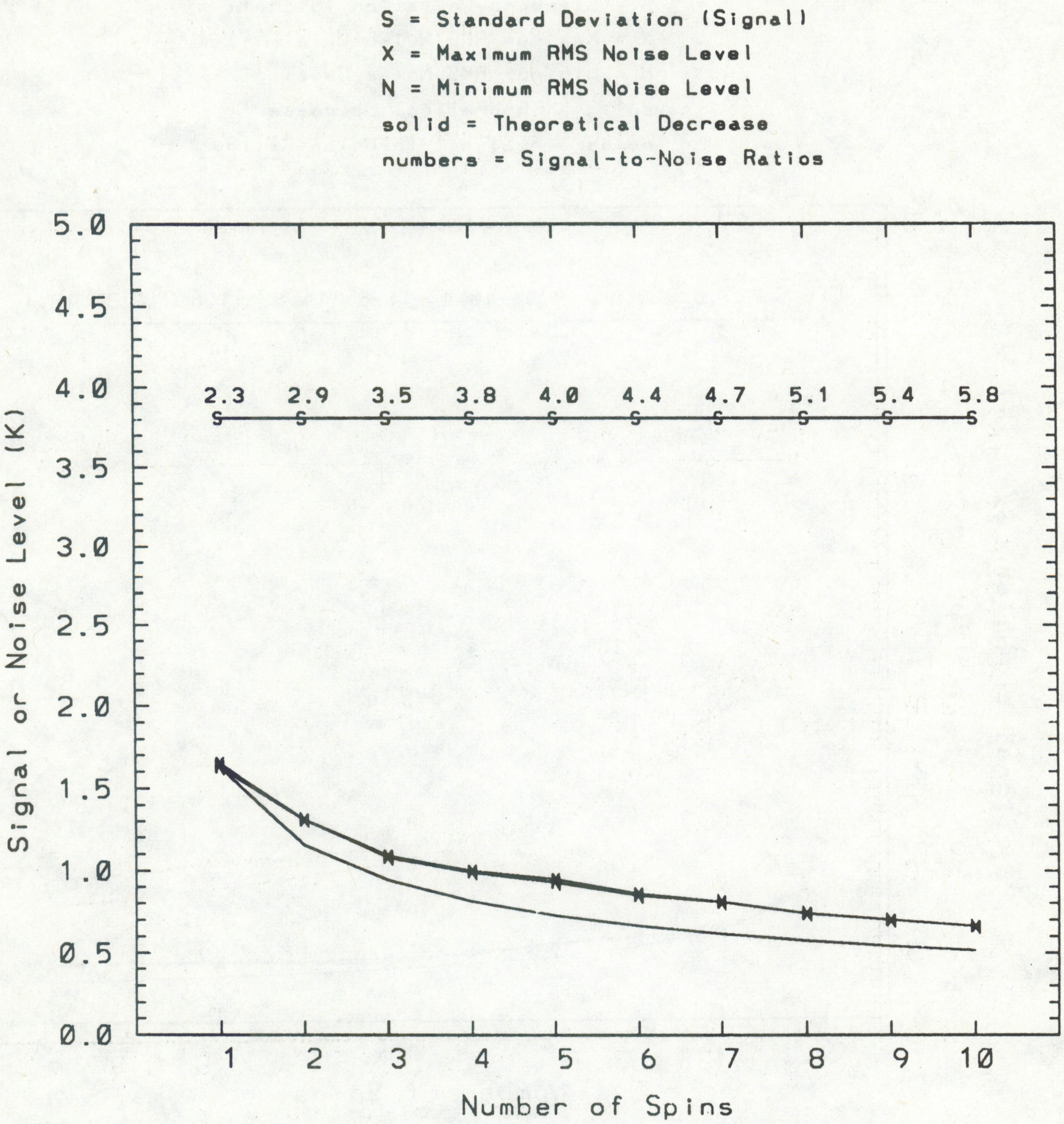

Figure 5d: Same as Figure 5a, but for VAS channel 4.

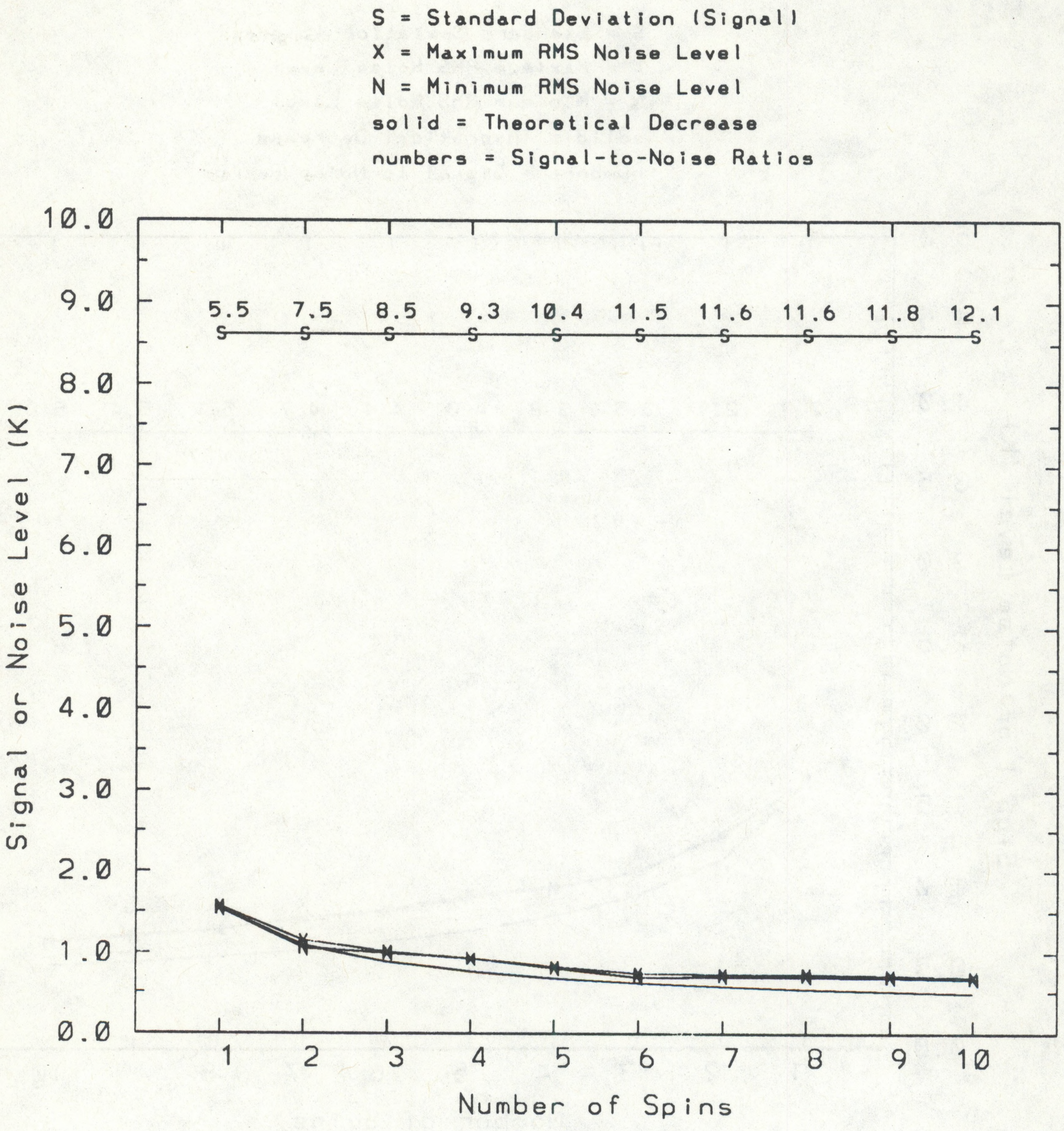

Figure 5e: Same as Figure 5a, but for VAS channel 5.

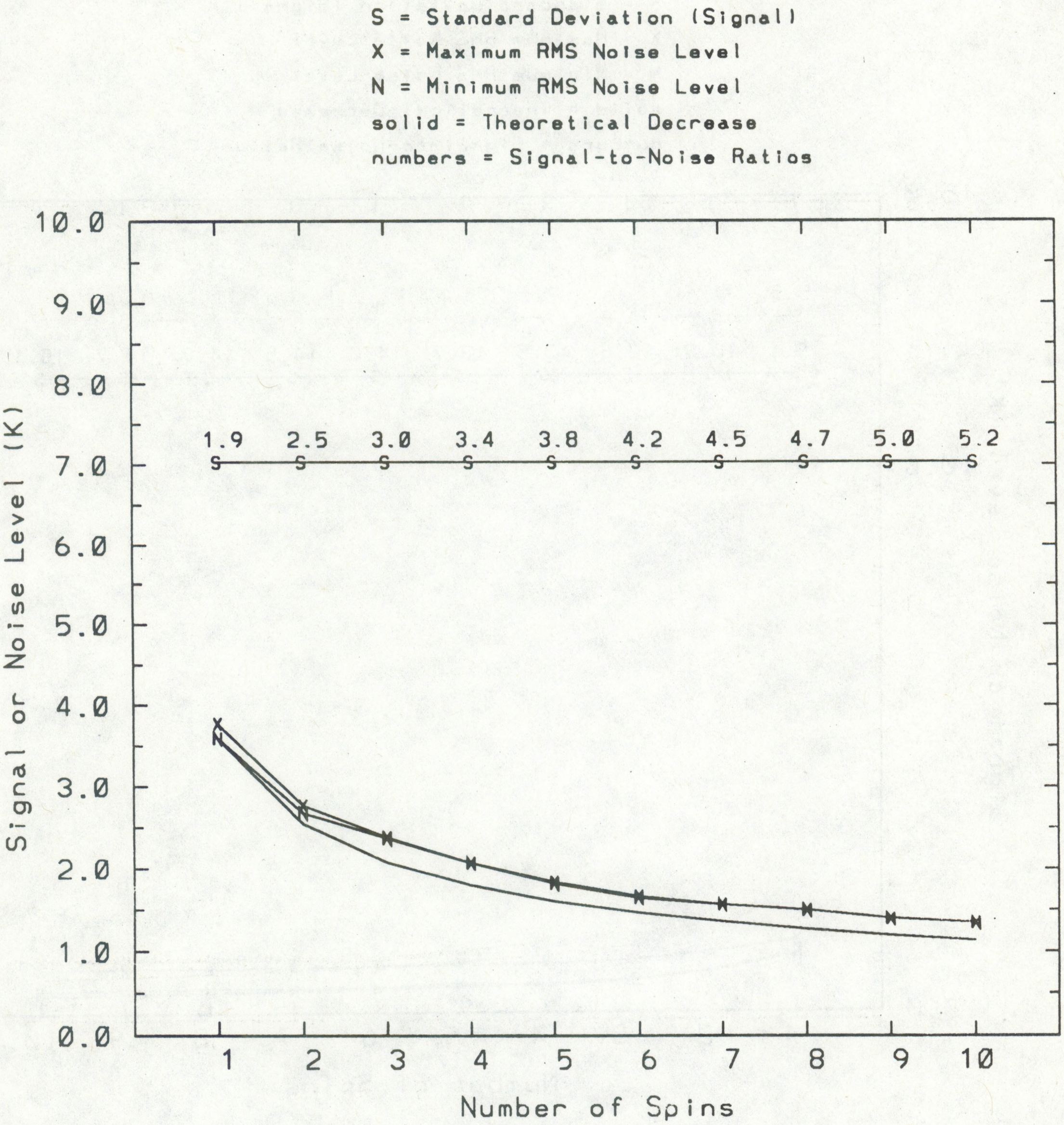

Figure 5f: Same as Figure 5a, but for VAS channel 6.

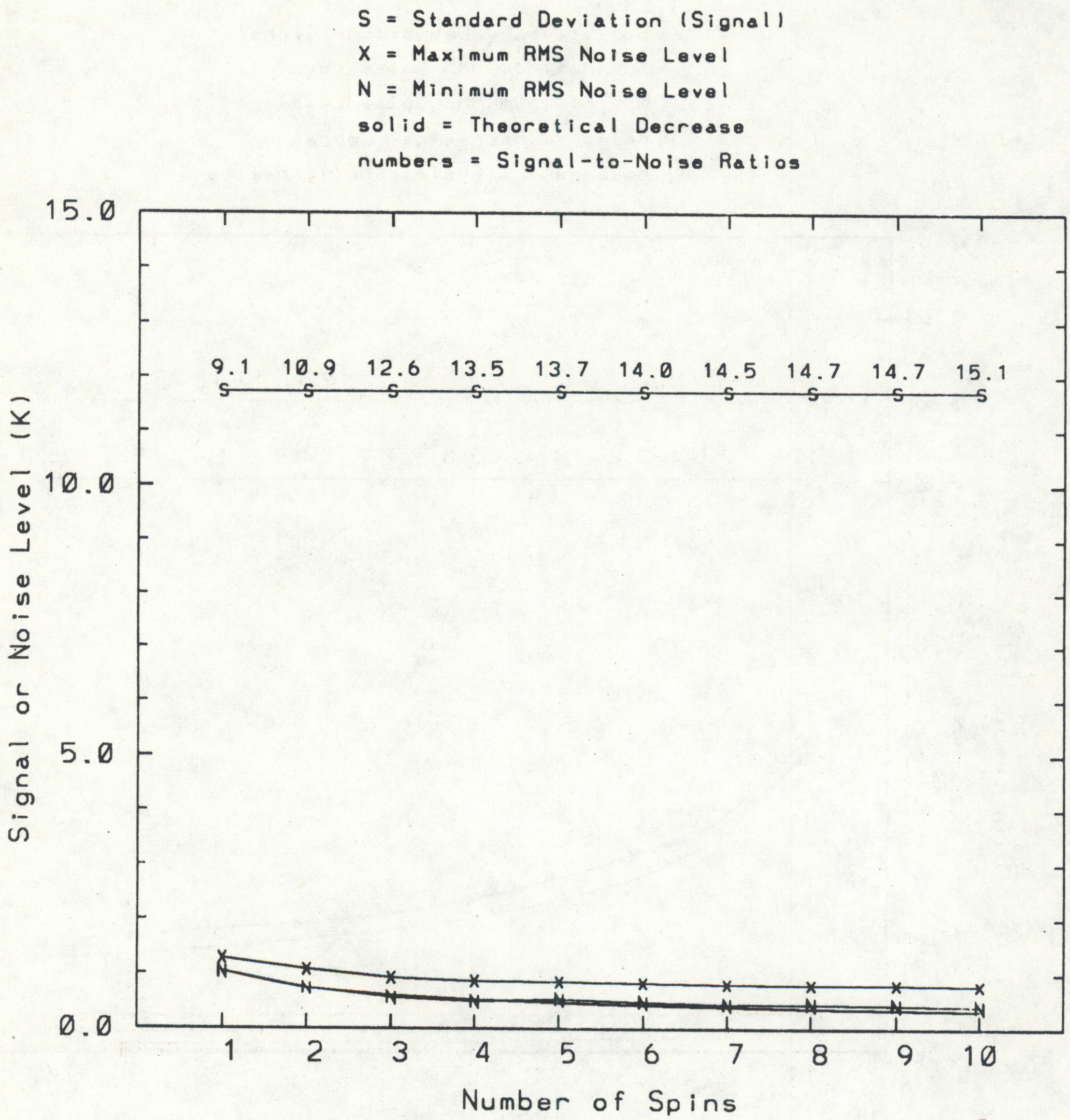

Figure 5g: Same as Figure 5a, but for VAS channel 7.

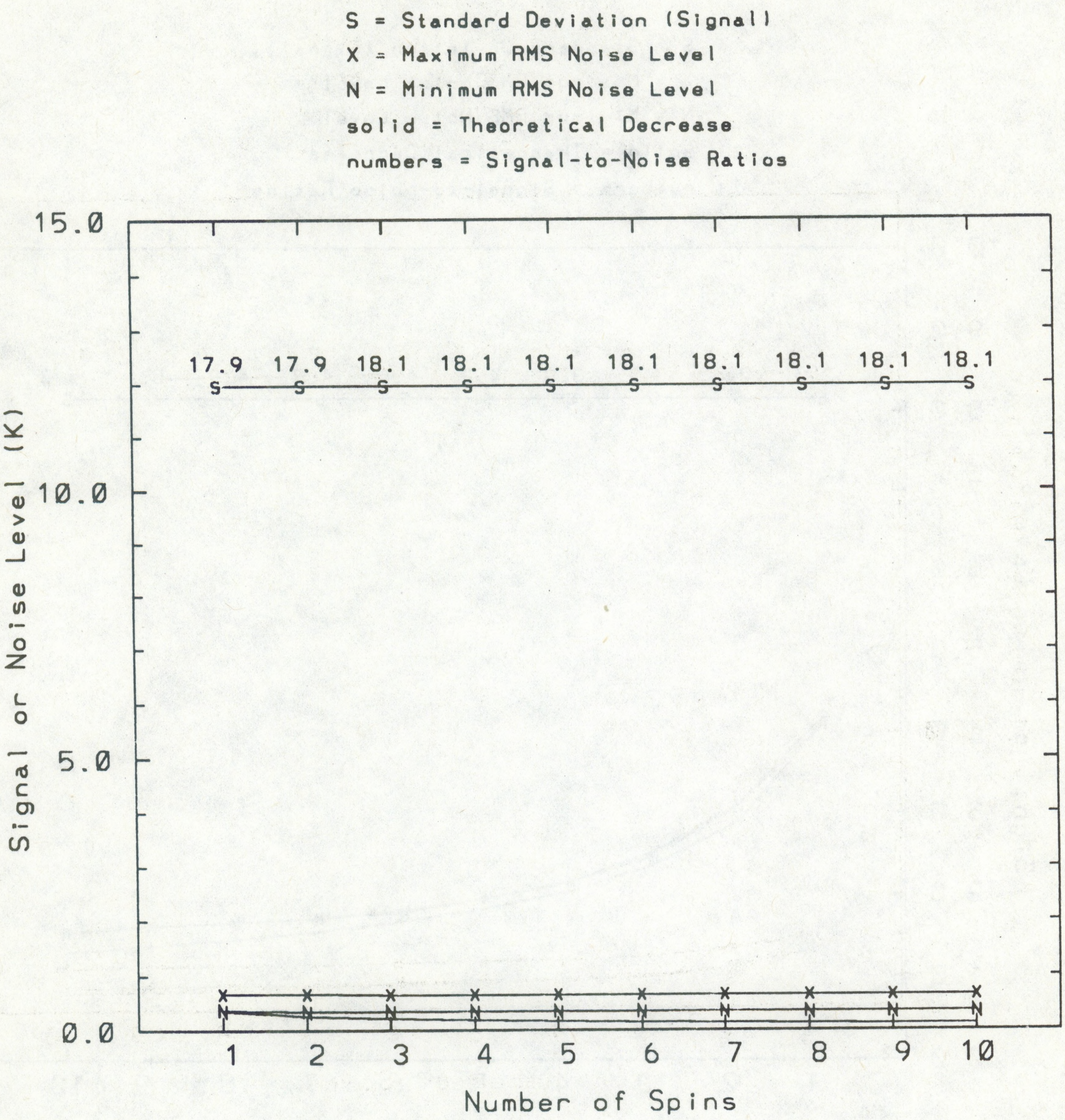

Figure 5h: Same as Figure 5a, but for VAS channel 8.

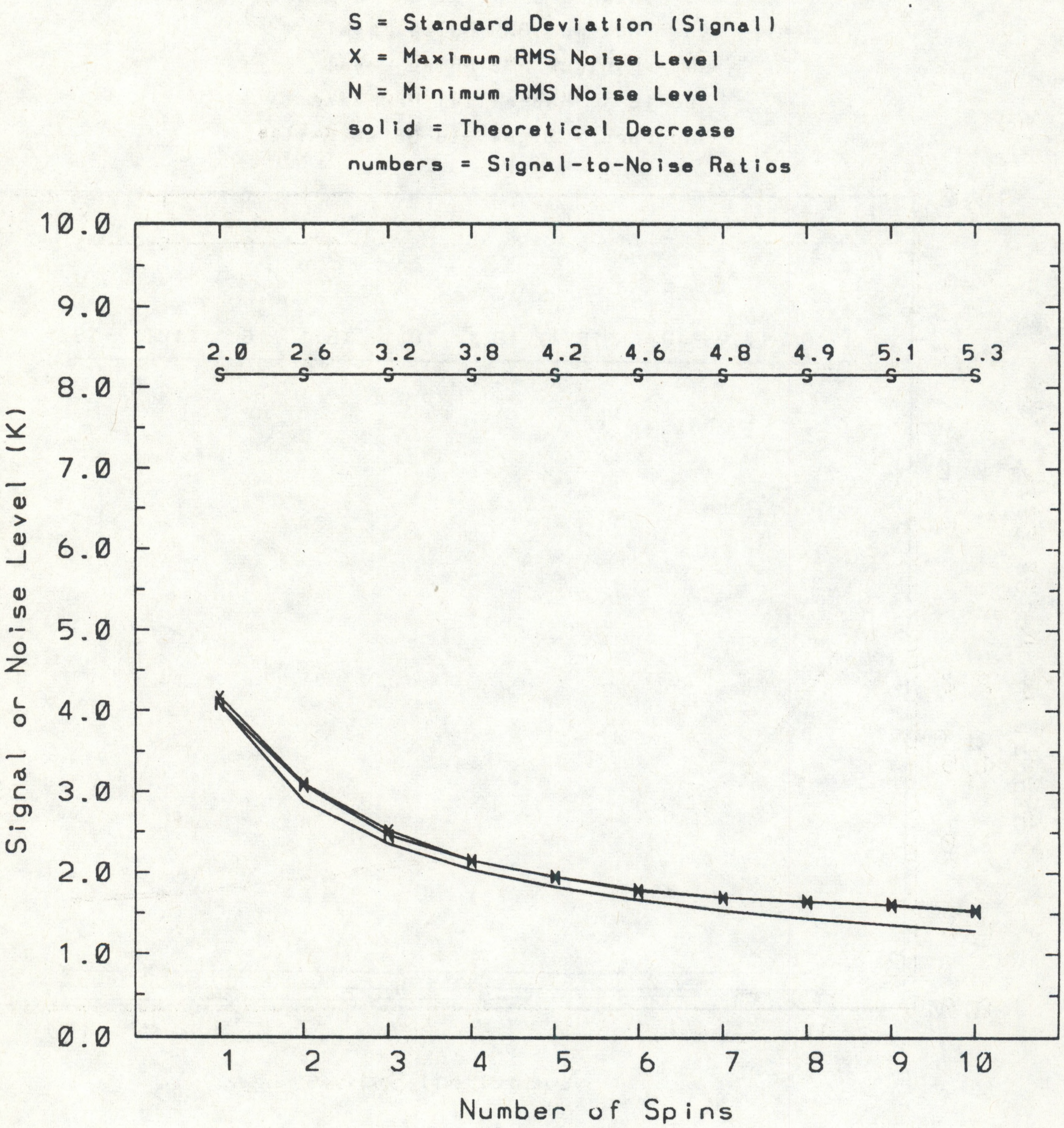

Figure 5i: Same as Figure 5a, but for VAS channel 9.

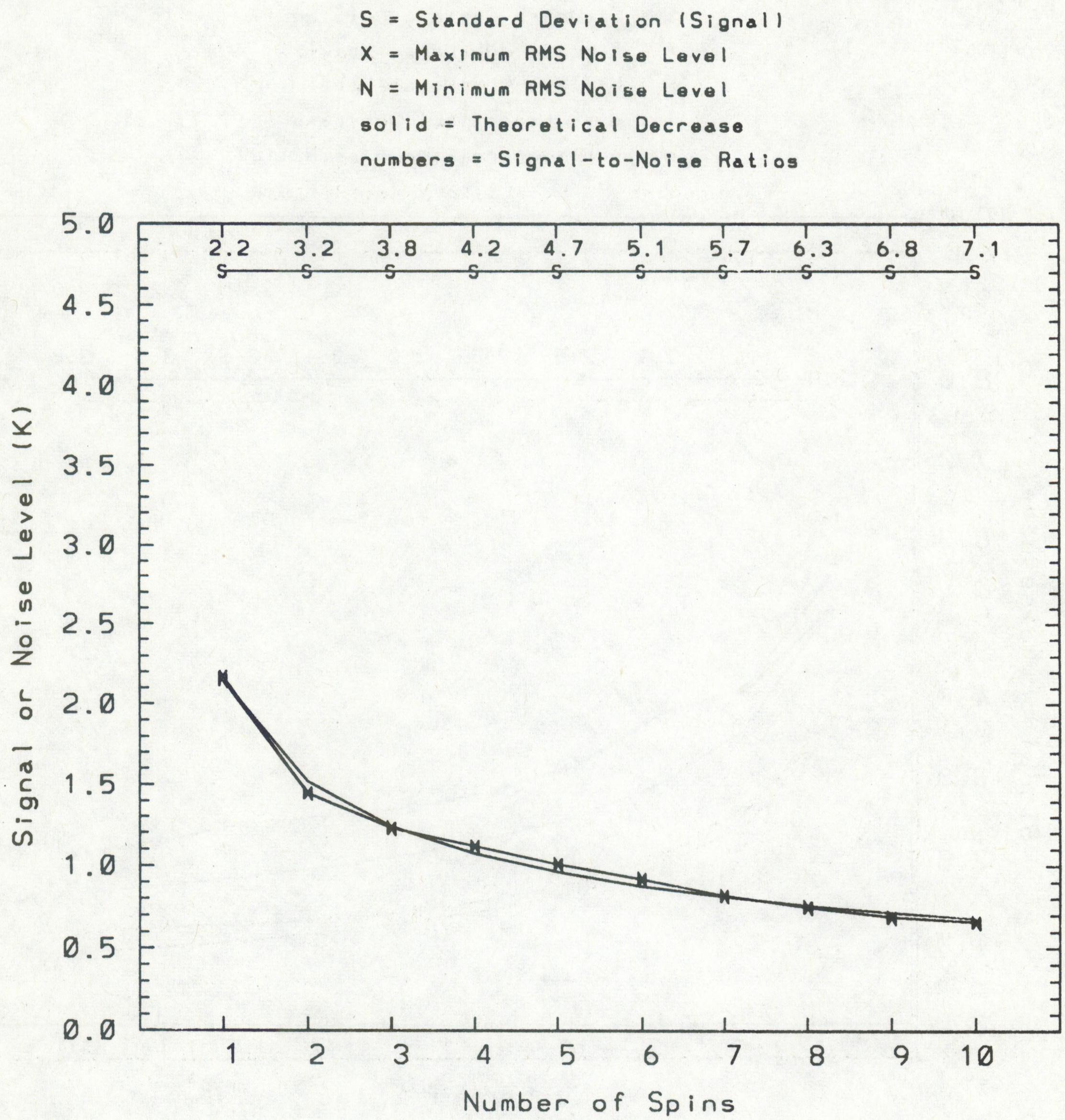

Figure 5j: Same as Figure 5a, but for VAS channel 10.

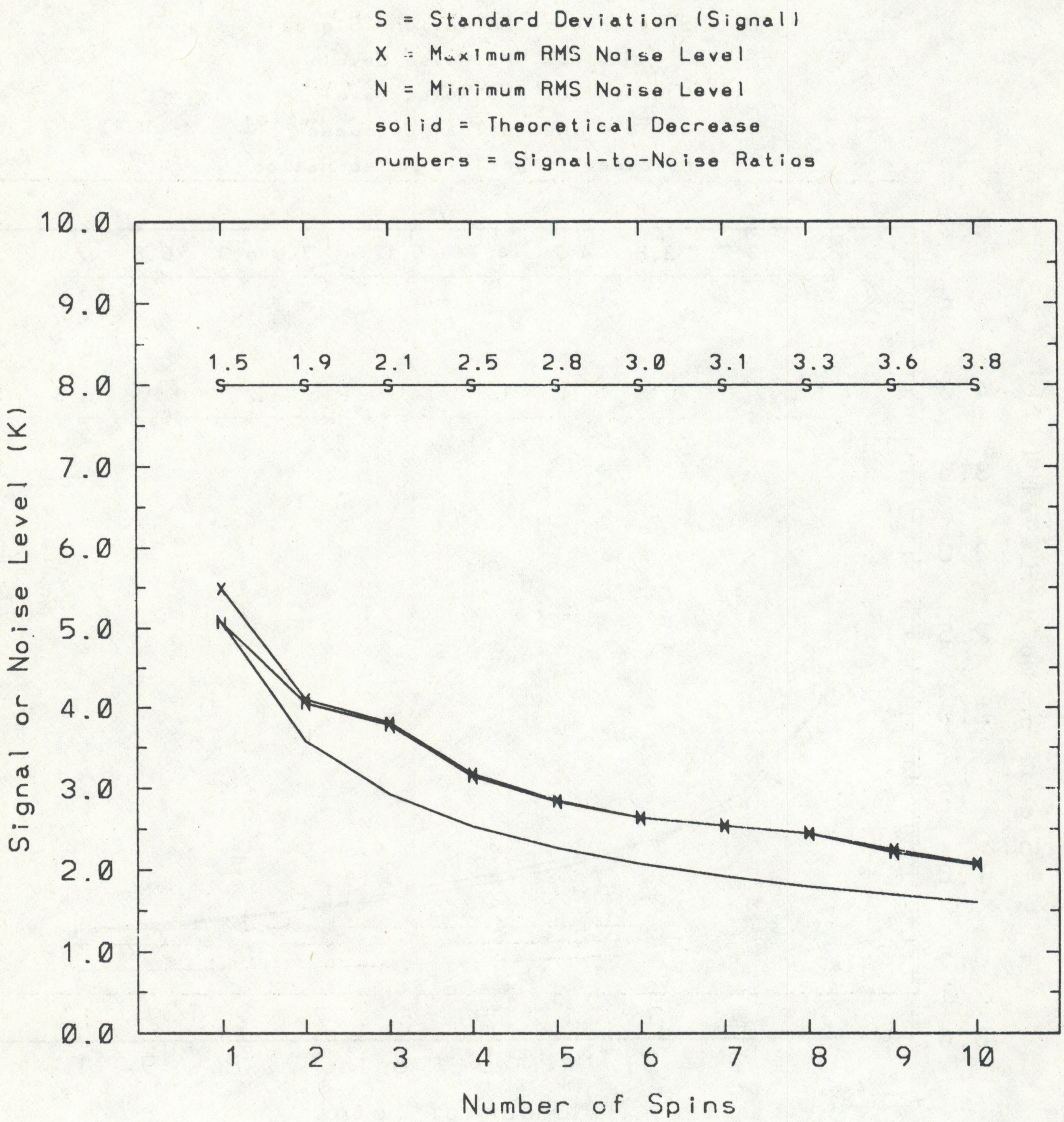

Figure 5k: Same as Figure 5a, but for VAS channel 11.

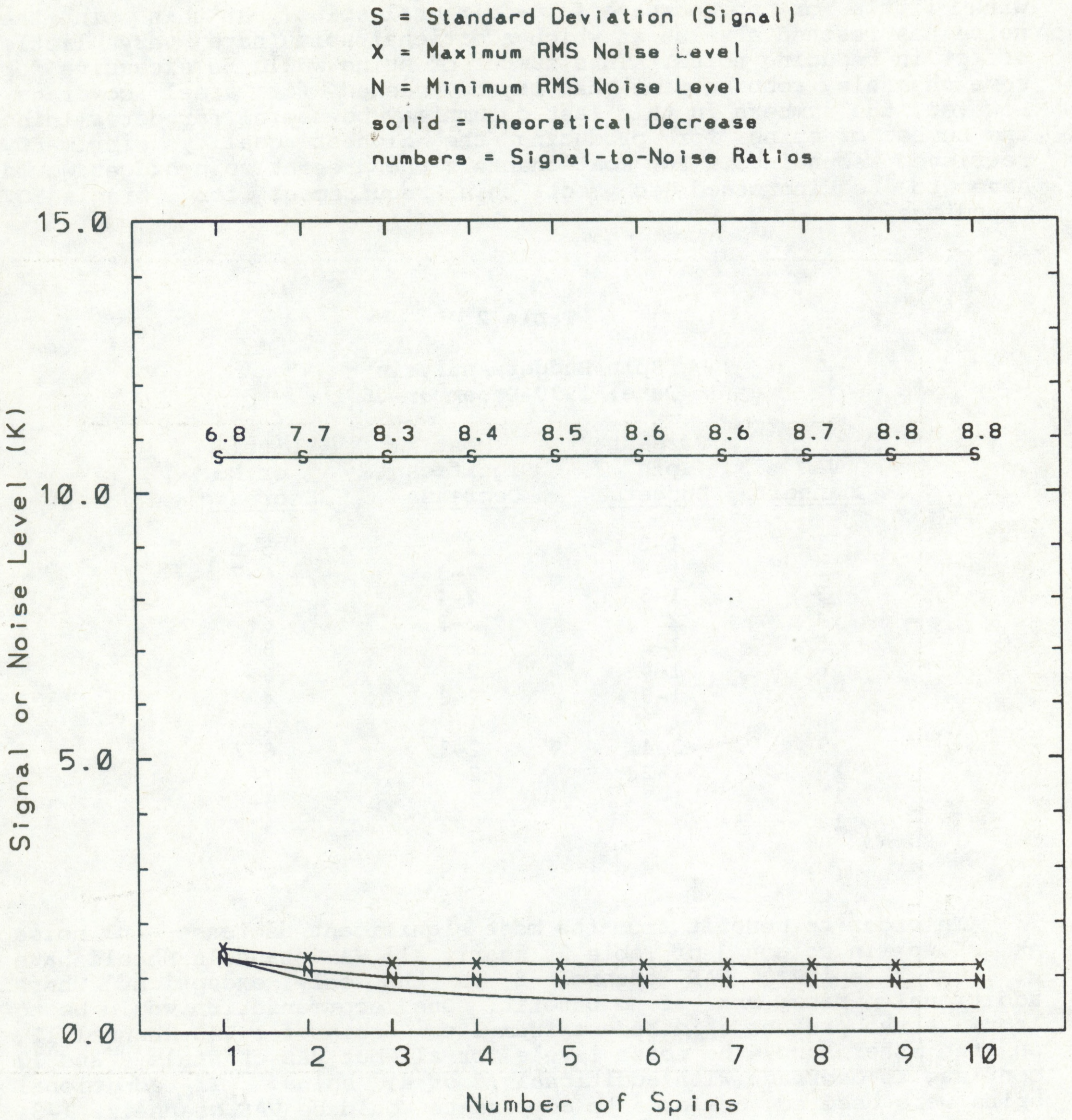

Figure 51: Same as Figure 5a, but for VAS channel 12.

is the number of spins required for the noise to reach a stable level with little or no decrease for additional spins. At this point the noise has reached a value at which additional spins have very little effect in reducing noise. This number of spins would be excessive for some channels, robbing time that may be needed for areal coverage. However, the numbers in this last column may be useful for determining the number of spins for producing the highest quality single-FOV retrieved soundings. For most channels the present spin budget would have to be increased to meet this requirement for single-FOV soundings.

Table 2

Spin Budget Analysis
Date: 1990-December-06

VAS Channel	Present Spin Budgets	Most Significant Decrease	Little or No Decrease
1	1-2	2	5-8
2	1-3	2-3	6-7
3	1-3	2-4	5-7
4	2	2-3	6+
5	1-2	2	6
6	1-4	2	6+
7	1-3	2-3	4
8	1	1	1
9	2-4	2-3	6-7
10	1-2	2	7+
11	1-3	2	6+
12	1	2-3	3

In order to benefit from the most significant decrease in noise as shown in column 3 of Table 2, nearly all VAS channels should have at least 2 spins. VAS channel 8 is the only exception, where additional spins are of no benefit. One recommendation would be to increase the present spin budget from 1 to 2 spins for VAS channel 12. On the other hand, the noise levels for all but VAS channels 8 and 12 continue to decrease with additional (3 or 4) spins. If additional spins were desired, one area to compensate would be VAS channels (1-3) which measure in the stratosphere and upper troposphere, where gradients are generally weak or nonexistent on smaller scales. For these VAS channels one spin is enough to measure larger scale features. Spatial averaging can be used to compensate for high noise levels due to small numbers of spins. Recommendations therefore include zero or very low spin budgets for these VAS channels. For example VAS channel 1 could be eliminated (0 spins) and VAS channel 2 and possibly channel 3 could be collected with only 1 spin. All other VAS channels, except 8, should be collected with a minimum of 2 spins (the minimum numbers in column 3 of Table 2).

4.0 REPEAT-VIEW VARIABILITY

Besides the structure analysis, another measure of the noise levels of the VAS channels was obtained by statistically comparing the variability of measurements at a single FOV. This method is not possible with operational data, because the individual measurements (samples) for each spin are not normally saved. However for this special data set, individual measurements were saved in single-sample files and were statistically analyzed to determine the variability of the measurements in each of the VAS channels.

Because 10 spins (samples) were taken, it was possible to compute the standard deviation of the 10 samples. Statistics for all FOVs were combined by first subtracting the average value at each FOV. This was done to eliminate any spatial variability due to horizontal gradients across the analysis area. The resulting statistic is called the repeat-view variability since it is a measure of the variability of the single-sample (1-spin) measurements at any FOV. Also, by adding together groups of 2 spins at a time, it is possible to compute the variability of 5 independent samples of 2-spin averaged measurements. Likewise if 5 spins at a time are averaged together, it is possible to compute the variability of 2 independent samples of 5-spin averaged measurements. However, it is not possible to form 2 independent samples of more than 5 spins out of only 10 available spins. Two samples of 6 spins would have one spin in common, and are not statistically independent. The extreme but more clear situation would be the complete overlap in trying to form 2 samples of 10 spins at a time. Results from this analysis for 1, 2, and 5 spins are shown in Table 3 and are compared below to the equivalent structure-estimated noise levels.

Table 3

Repeat-view Noise Levels
Date: 1990-December-06

VAS Channel	1-spin Variability (K)	2-spin Variability (K)	5-spin Variability (K)
1	4.55	3.01	1.48
2	2.35	1.58	0.77
3	2.64	1.78	0.91
4	1.67	1.10	0.58
5	1.46	0.98	0.51
6	3.31	2.19	1.12
7	1.08	0.73	0.38
8	0.16	0.11	0.053
9	4.13	2.78	1.36
10	1.98	1.31	0.66
11	5.90	3.93	1.97
12	0.89	0.59	0.27

As expected, there is a decrease in noise level with increasing numbers of spins (samples), as was the case for the structure analysis. The repeat-view noise levels are plotted in Figures 6a through 6l for VAS channels 1 through 12. The line labeled 'R' in each graph is the repeat-view noise computed at 1, 2, and 5 spins per channel. For comparison purposes the theoretical decrease in noise with increasing numbers of spins is plotted as a solid line on each graph, as in Figure 5. The theoretical curves start with the value for 1 spin and use Equation 2 to compute the values for 2 and 5 spins. For all VAS channels the measured and theoretical curves are similar, showing that the noise does decrease as expected. However, in all cases the measured decrease in noise level is greater than the theoretical decrease at 2 and 5 spins. This is just opposite of what was true for the structure-estimated results, where the measured decrease in noise was less than predicted by theory.

5.0 SPACE-VIEW VARIABILITY

During the special VAS data collection period, NESDIS/CIMSS computed the variability of space-view (well off the edge of the Earth) measurements (Menzel and Schmit, 1990). Table 4 lists the space-view results. For each VAS channel the number of spins is given in column 2. For all VAS channels, the space-view variability was measured as the standard deviation of about 2000 10-spin averaged measurements. Because 10 spins were collected, the average variability in columns 4 and 5 of Table 4 is the single-sample noise reduced by 10 spins. These numbers were then converted into the single-sample noise levels in columns 6 and 7 using the inverse of Equation 2. This is the single-sample noise assuming that noise increases as the square root of the number of samples. Columns 4 and 5 are measured values, whereas columns 6 and 7 are derived values. Note also that the noise levels are given both in radiance units (mW/[m^2 sr cm^{-1}]) and in temperature units (kelvin). The conversion from radiance (L) variability to temperature (T) variability uses the formula

$$DT = DL/(dB[j,\overline{T}]/dT), \qquad (3)$$

where dB/dT is the derivative of the Planck function (B) at the given wavelength (or channel, j) and the average radiance (or temperature, $\overline{T}$) at that wavelength. The average radiances used in Equation 3 are listed in column 3 of Table 4. Care was taken to use appropriate average radiances to make the radiance to temperature conversion since the derivative of the Planck function is highly temperature dependent. The average radiances used are the mean values measured in each VAS channel for this special data set. The resulting space-view noise levels in temperature units are compared below to both the structure-estimated noise levels and the repeat-view variabilities.

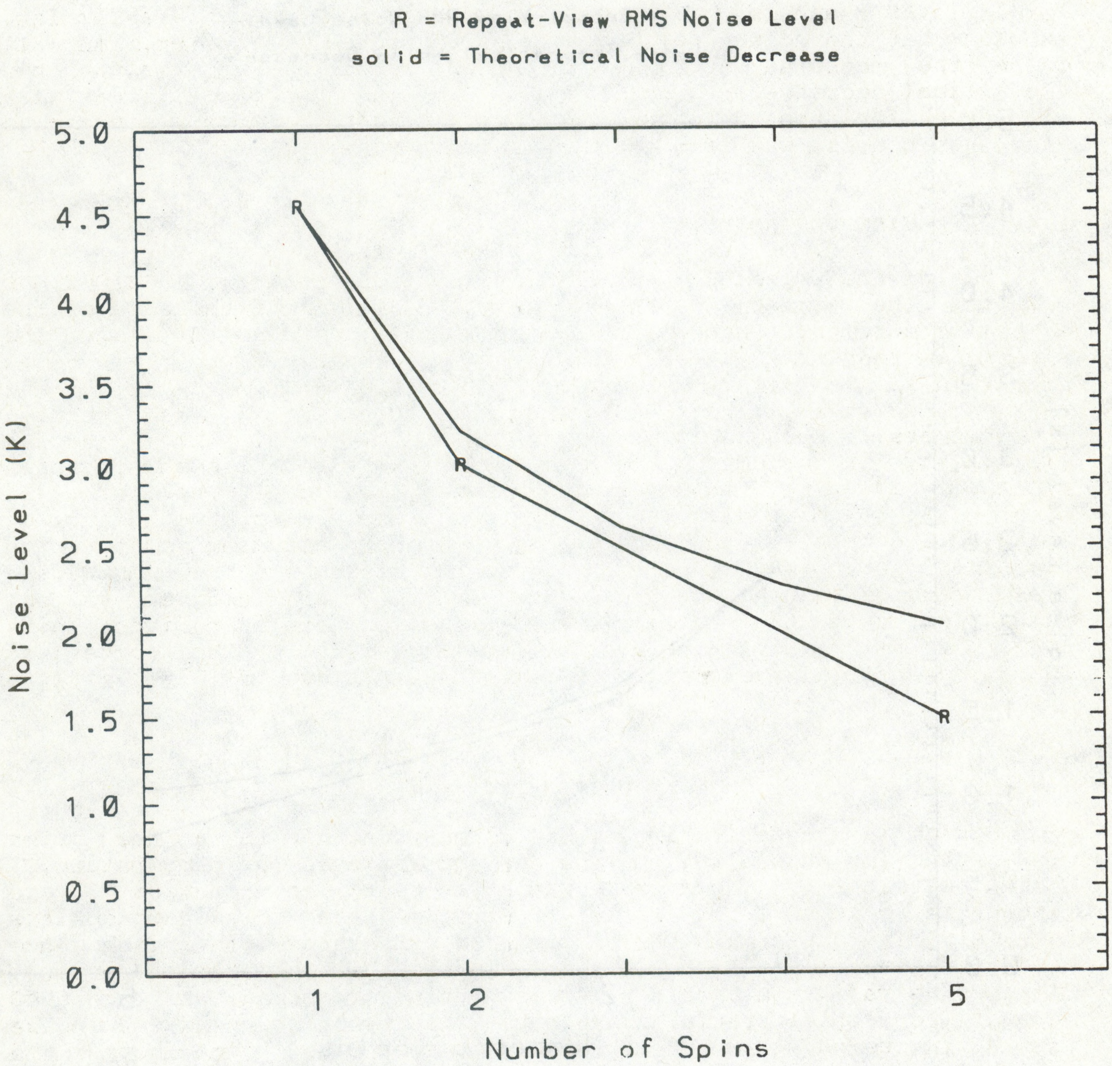

Figure 6a: Repeat-view noise level as a function of the number of spins for VAS channel 1. The line labeled 'R' is the noise level for 1, 2, and 5 spins. The unlabeled solid line is the theoretical decrease in noise level with increasing number of spins (samples).

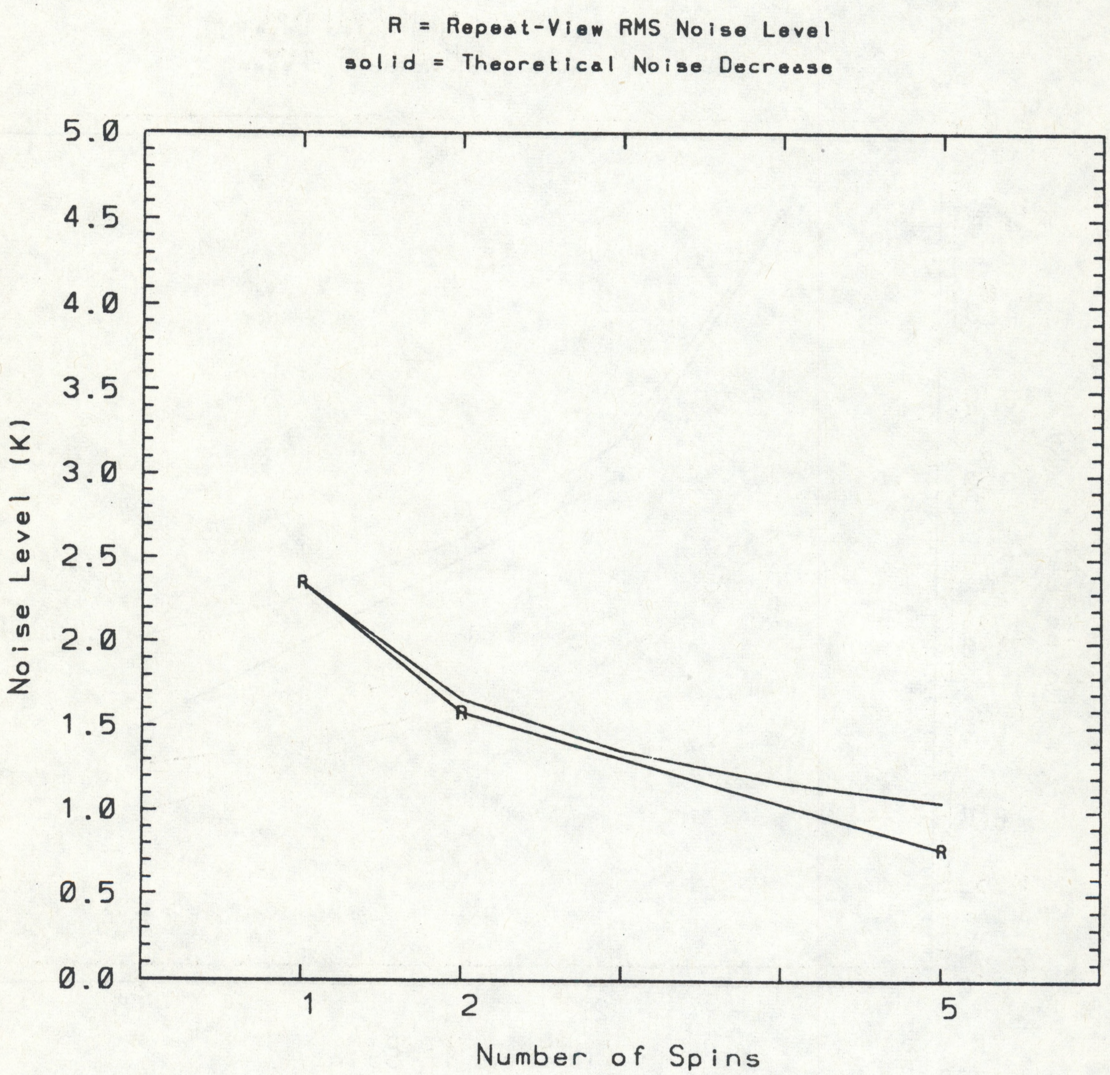

Figure 6b: Same as Figure 6a, but for VAS channel 2.

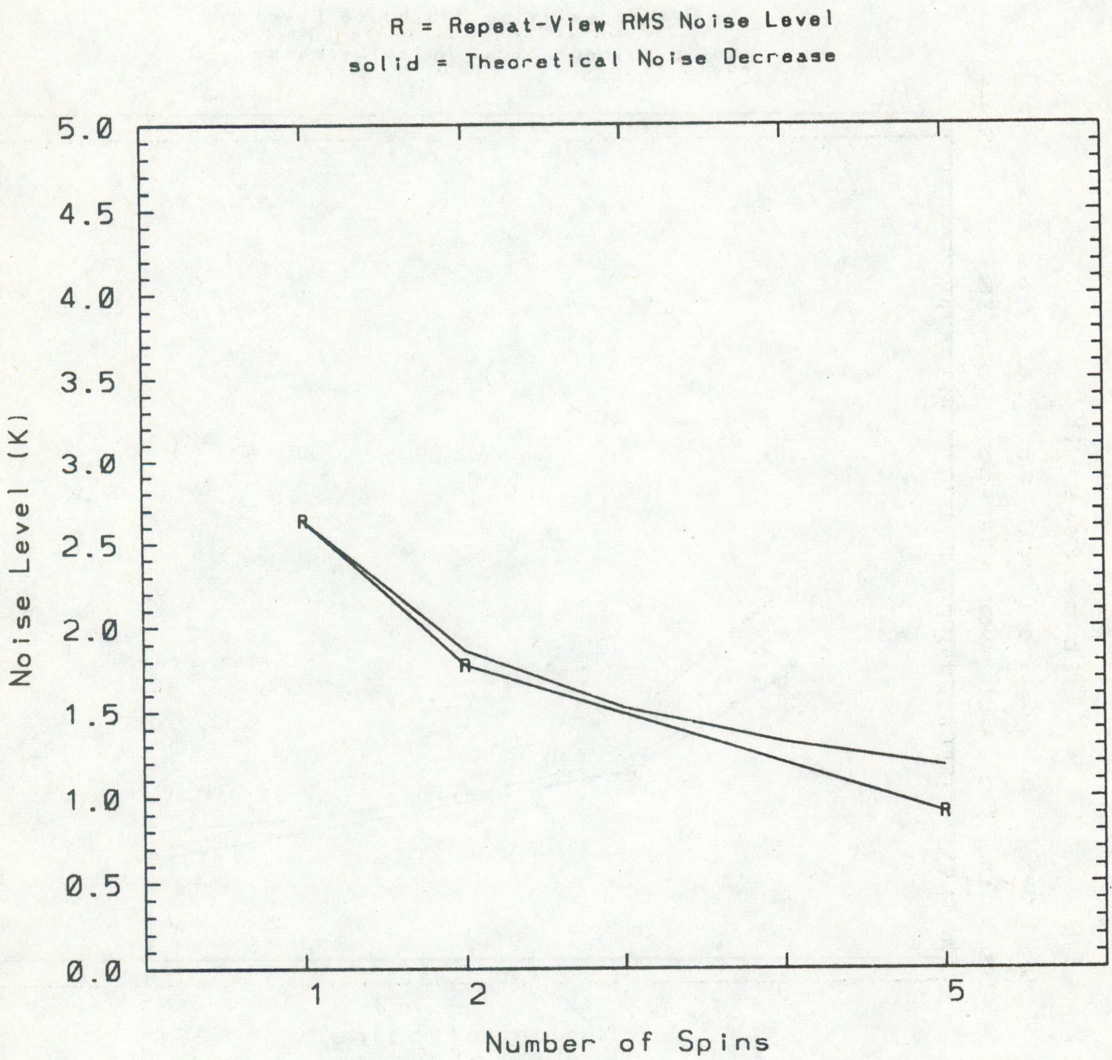

Figure 6c: Same as Figure 6a, but for VAS channel 3.

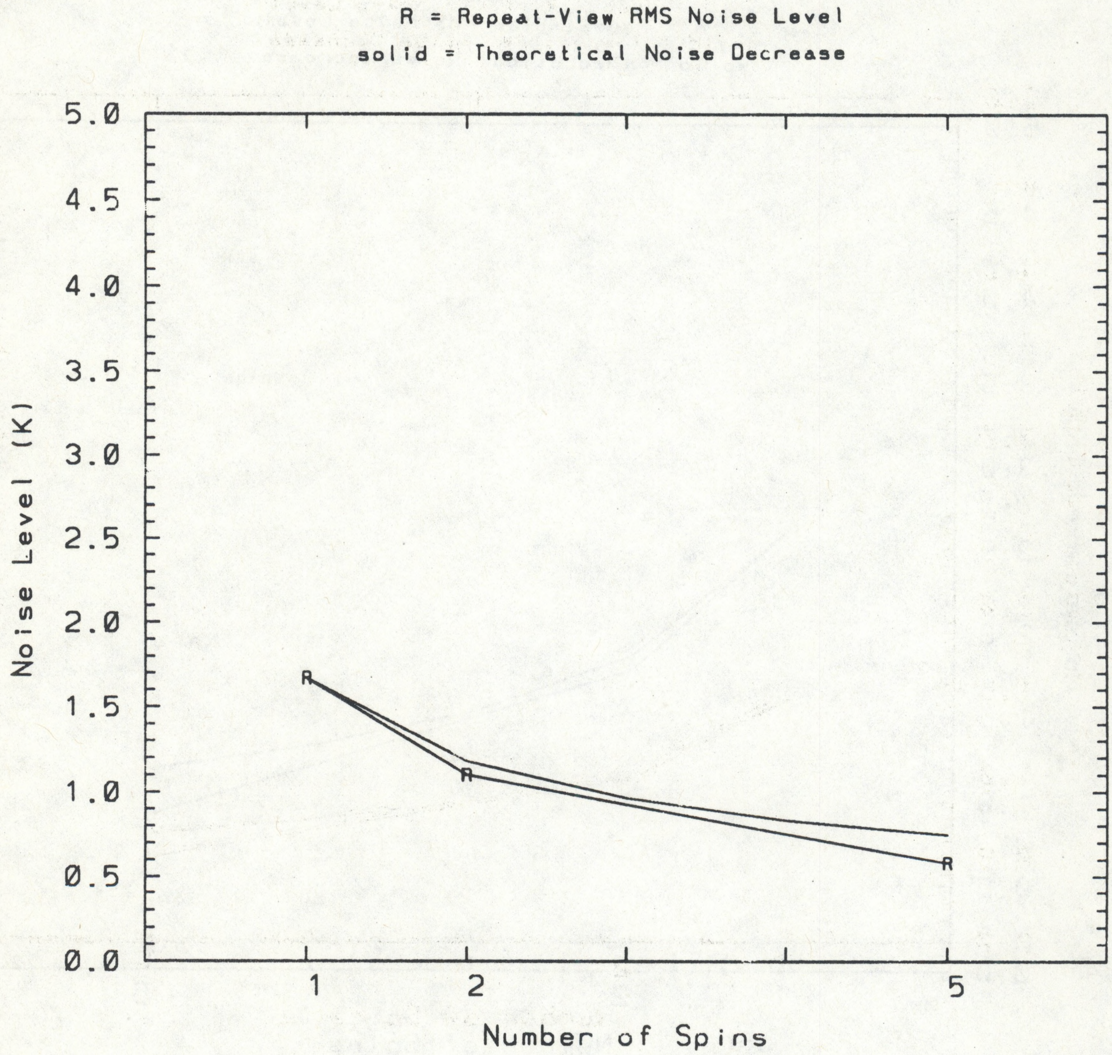

Figure 6d: Same as Figure 6a, but for VAS channel 4.

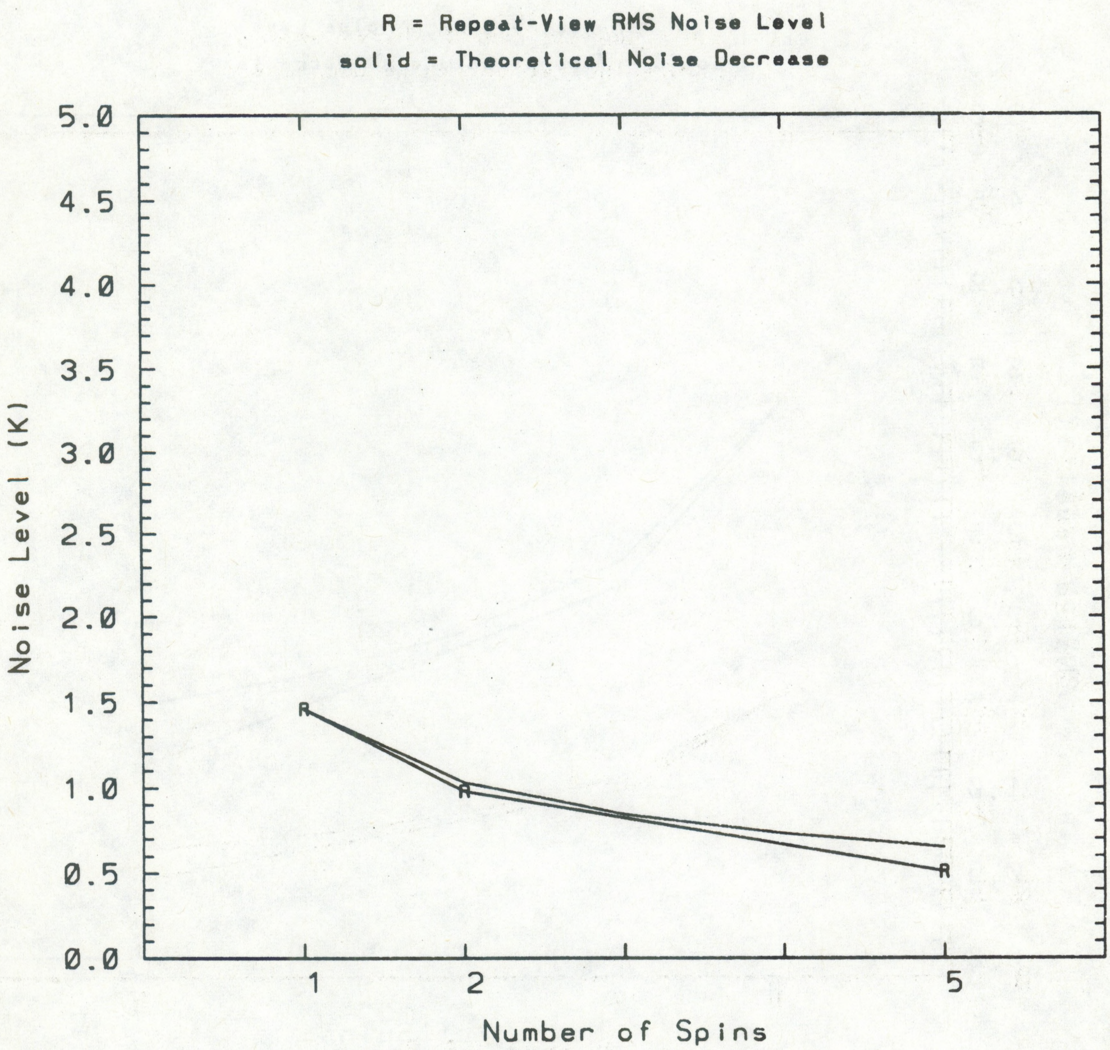

Figure 6e: Same as Figure 6a, but for VAS channel 5.

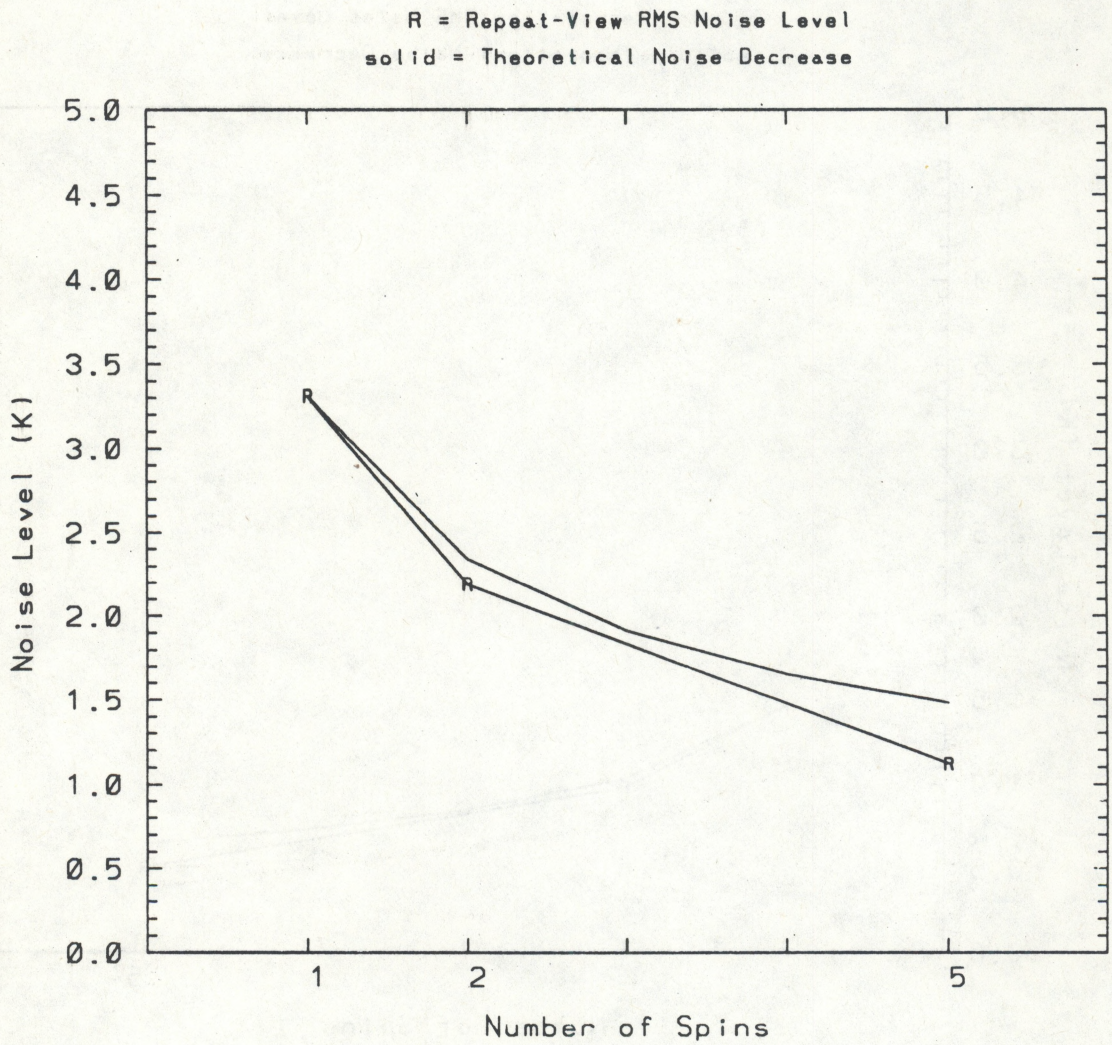

Figure 6f: Same as Figure 6a, but for VAS channel 6.

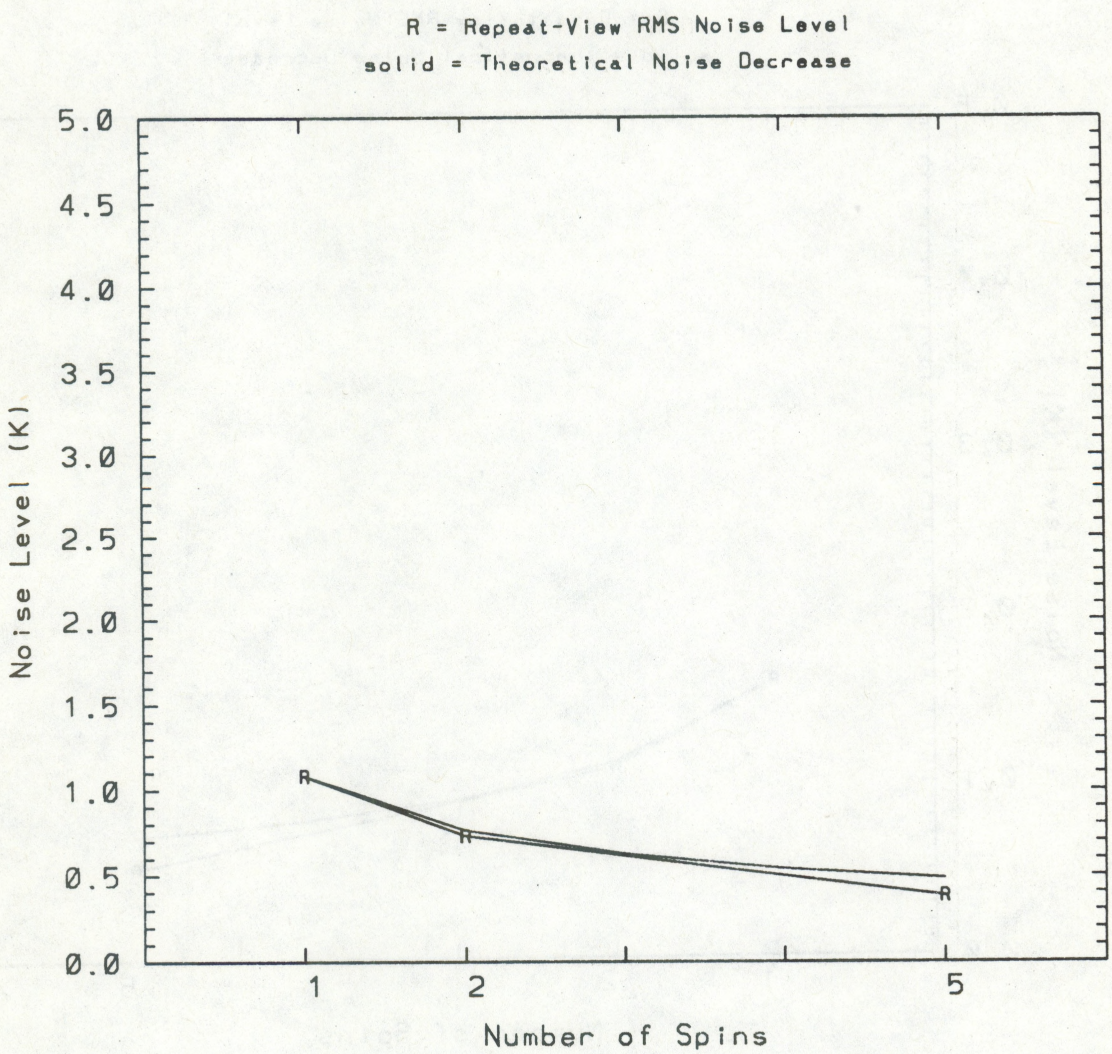

Figure 6g: Same as Figure 6a, but for VAS channel 7.

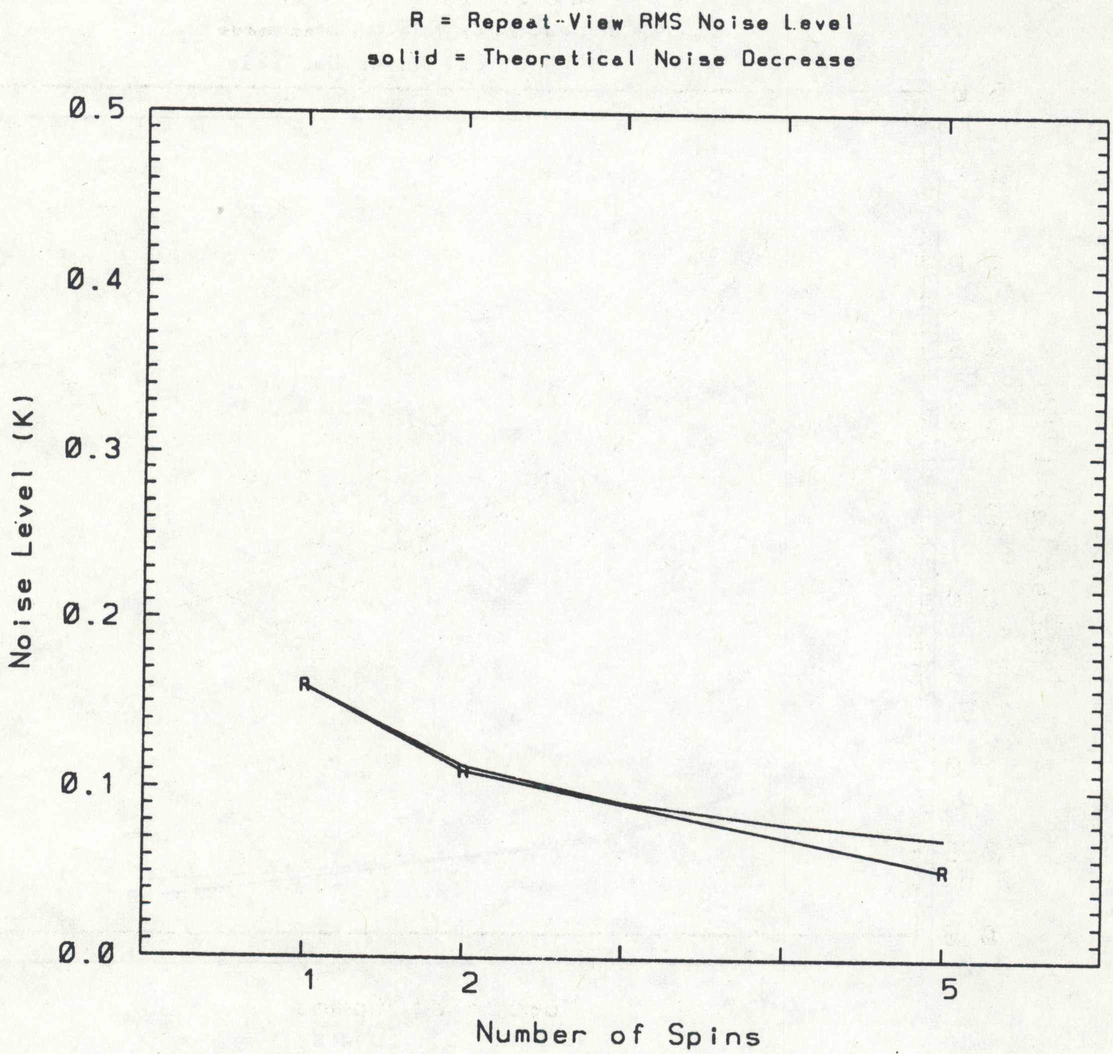

Figure 6h: Same as Figure 6a, but for VAS channel 8.

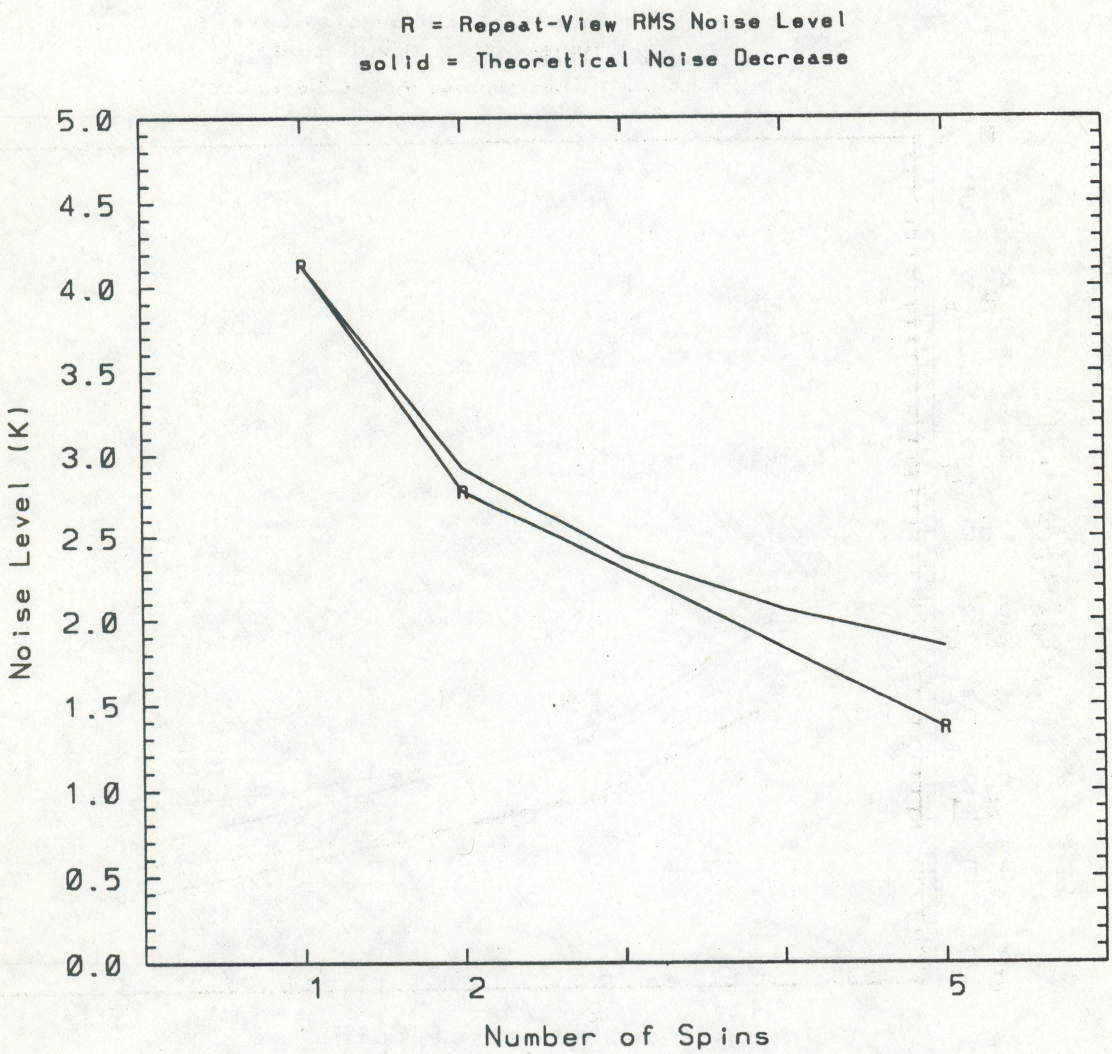

Figure 6i: Same as Figure 6a, but for VAS channel 9.

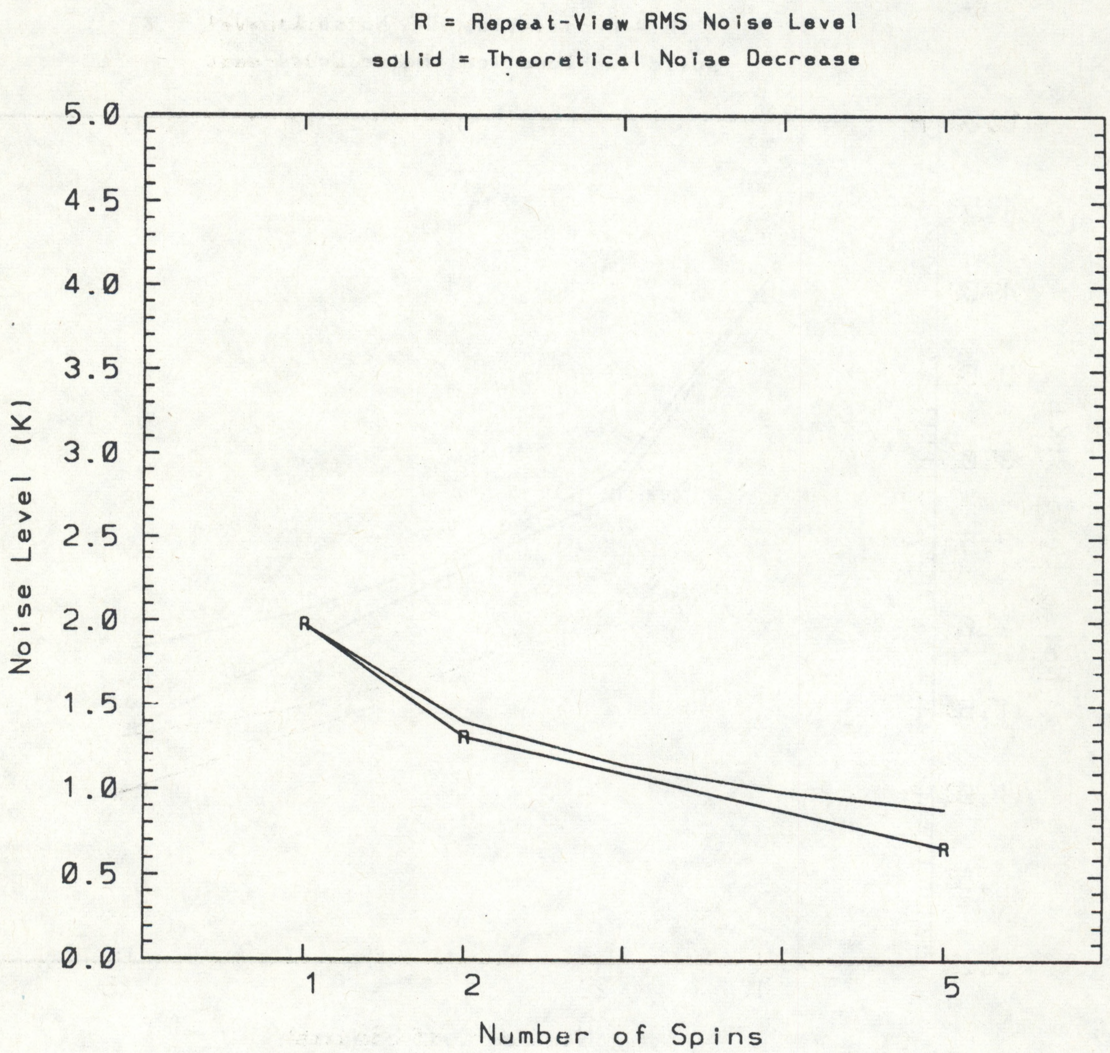

Figure 6j: Same as Figure 6a, but for VAS channel 10.

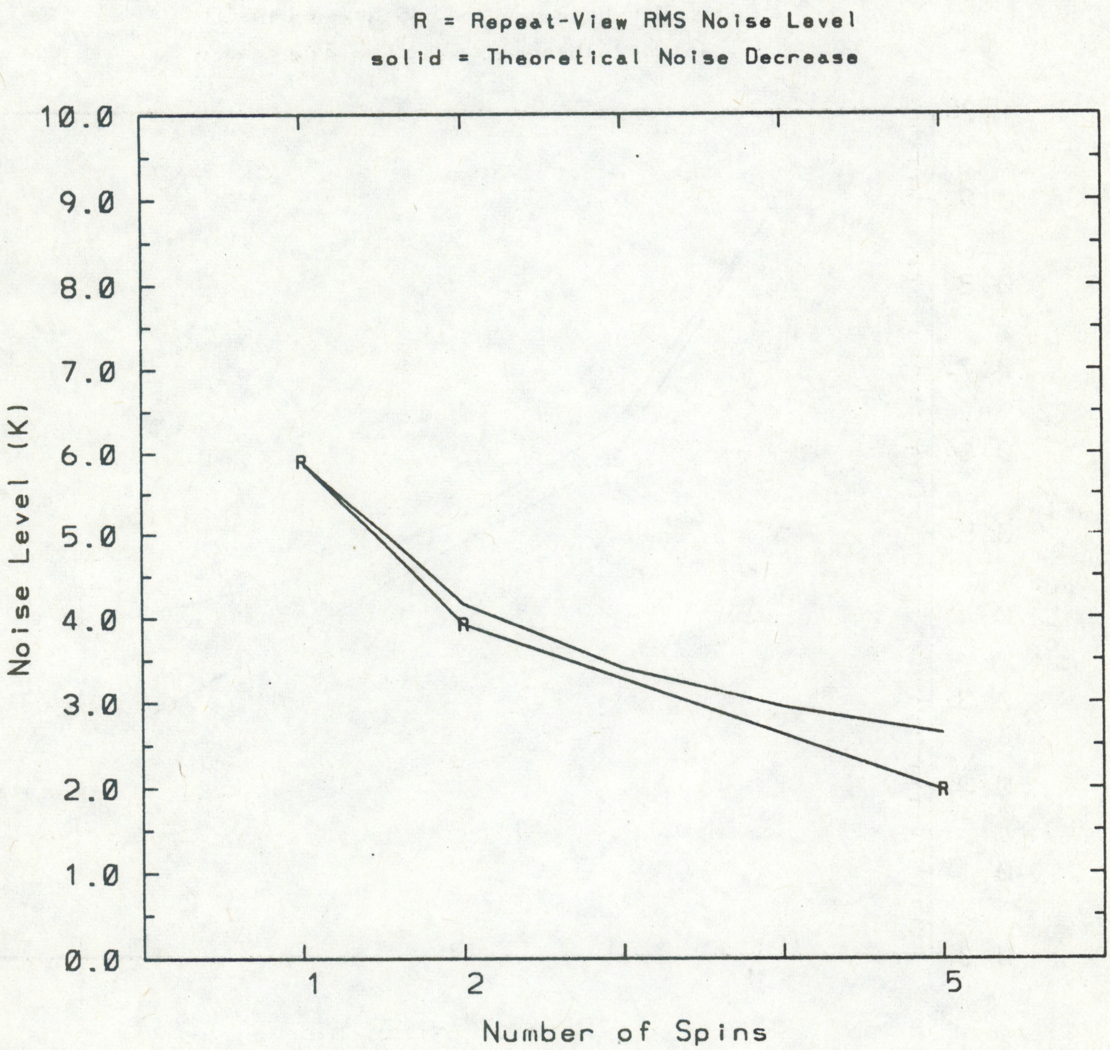

Figure 6k: Same as Figure 6a, but for VAS channel 11.

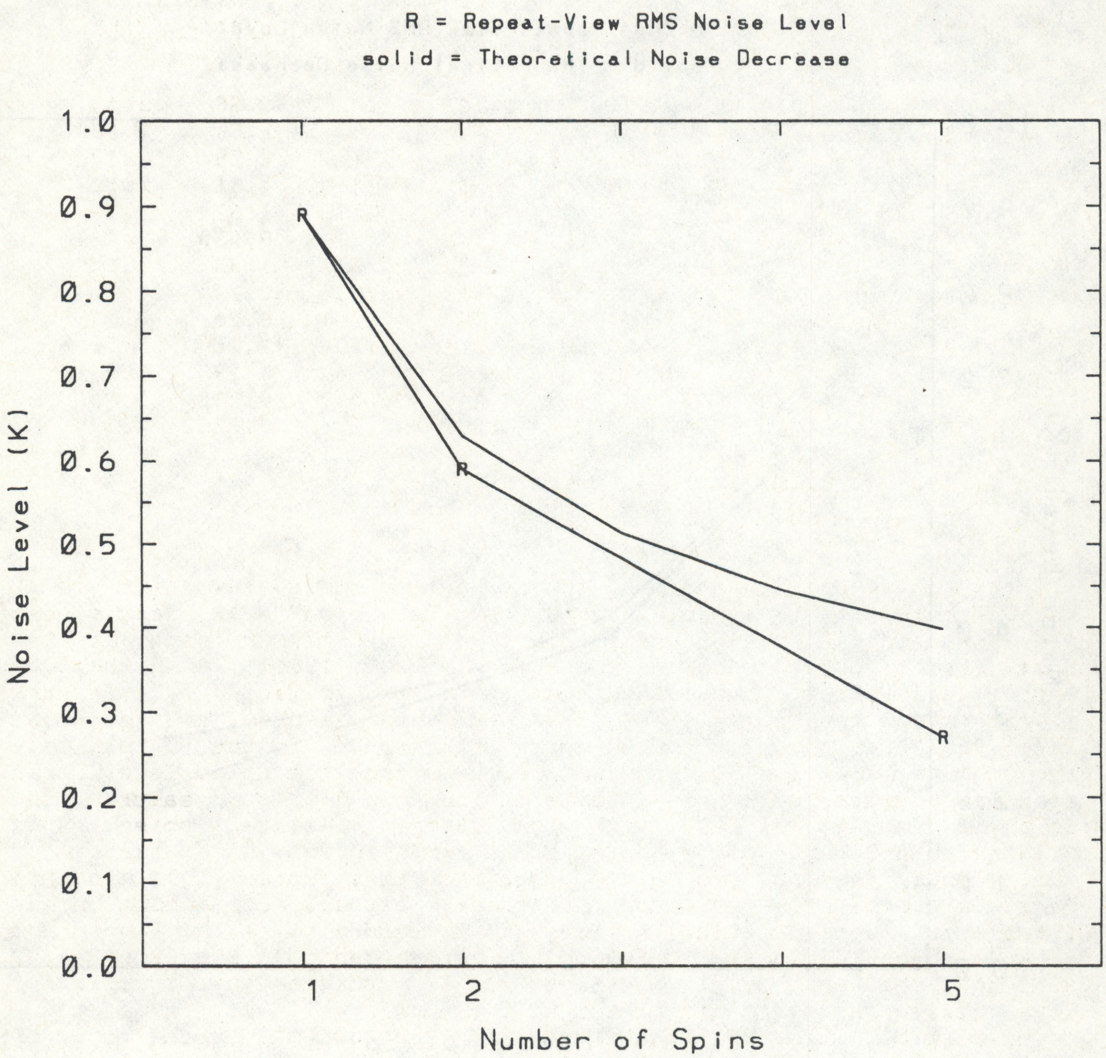

Figure 6l: Same as Figure 6a, but for VAS channel 12.

Table 4

Space-view Noise Levels
Date: 1990-December-18

VAS Channel	Number of Spins	Average* Radiance (mW/..)	10-spin Variability (mW/..)	10-spin Variability (K)	1-spin Variability (mW/..)	1-spin Variability (K)
1	10	52.	1.70	1.72	5.38	5.43
2	10	49.	0.81	0.84	2.56	2.66
3	10	48.	0.72	0.75	2.28	2.37
4	10	53.	0.51	0.50	1.61	1.58
5	10	68.	0.51	0.43	1.61	1.35
6	10	0.22	0.0096	0.78	0.030	2.43
7	10	75.	0.42	0.33	1.33	1.04
8(1-spin)	1	62.	0.044	0.038	0.14	0.12
8(10-spin)	10	62.	0.075	0.064	0.24	0.21
9	10	10.	0.40	1.20	1.26	3.79
10	10	4.4	0.092	0.54	0.29	1.71
11	10	0.19	0.012	1.01	0.038	3.49
12	10	0.30	0.0026	0.18	0.0082	0.55

* radiance units are (mW/[m^2 sr cm^{-1}])

In the special case of VAS channel 8, two space-view noise level measurements are available, one for the normal VAS data stream (10-spin) and the other for a single spin from another part of the data stream (between scan mirror steps [Menzel, 1980]), when the scan mirror is stepping. Both situations are listed in Table 4. In the 1-spin case the noise level for 1 spin was measured, and the noise level for 10 spins was computed using Equation 2. In the 10-spin case the noise level for 10 spins was measured, and the noise level for 1 spin was computed using the inverse of Equation 2. The measured and computed results differ, with the 10-spin measured noise levels greater than the 10-spin computed noise levels by about a factor of two. Both results are given, showing that noise levels do not decrease exactly as expected by theory because non-random noise interferes (Menzel, 1980). For totally random noise the 1-spin and 10-spin noise levels should follow the relationship in Equation 2. In addition, the noise level in VAS channel 8 approaches the digitization level of the satellite signal for this channel. If the true noise level were below the digitization level, that would limit the accuracy of the measured radiances. For VAS channel 8 the digitization level for 1 measured count value is 0.24 mW/(m^2 sr cm^{-1}), which means that the noise level cannot be determined within plus or minus one half (0.12 mW/[m^2 sr cm^{-1}]) of the digitization level. This is close to the noise level measured at 1 spin (0.14 mW/[m^2 sr cm^{-1}]) in column 6 of Table 4. This may indicate that the measurements in VAS channel 8 are digitization limited.

6.0 COMPARISONS OF NOISE LEVELS TO DESIGN SPECIFICATIONS

The noise levels estimated by performing structure function analysis and computed from repeat-view statistics should be similar to those obtained from space-view 'calibration' data. Table 5 is a comparison of noise levels from these three analysis methods. Column 2 gives the structure-estimated noise levels, column 3 gives the repeat-view variability (from column 2 of Table 3), and column 4 gives the single-sample space-view variability (from column 7 of Table 4). In addition, the last column in Table 5 gives the pre-launch design specifications for single-sample VAS measurements (Chesters and Robinson, 1983; Chesters, et al, 1985). In each column the noise levels are for single-sample (1-spin) measurements.

Table 5

Single-sample (1-spin) Noise Level Comparison

VAS Channel	Structure Estimate (K)	Repeat-view* Variability (K)	Space-view** Variability (K)	Single-sample Design Specs (K)
1	4.50	4.55	5.43	5.3
2	2.44	2.35	2.66	2.2
3	2.61	2.64	2.37	1.8
4	1.63	1.67	1.58	1.2
5	1.54	1.46	1.35	1.0
6	3.60	3.31	2.43	1.6
7	1.04	1.08	1.04	1.0
8(1-spin)	0.37	0.16	0.12	0.1
8(10-spin)	0.37	0.16	0.21	0.1
9	4.08	4.13	3.79	3.4
10	2.15	1.98	1.71	1.6
11	5.07	5.90	3.49	6.7
12	1.37	0.89	0.55	0.8

* from Table 3, column 2
** from Table 4, column 7

Figure 7 is a bar graph of the same numbers as in Table 5. Vertical bars with different shading are used to compare the three noise level determinations to the pre-launch design specifications for each of the 12 VAS channels. The structure-estimated noise levels are unshaded. Repeat-view noise levels are shaded with vertical lines. Space-view noise levels are shaded with horizontal lines. The design specifications are shaded black.

Table 5 shows that the structure-estimated noise levels compare well with the repeat-view variability, with most differences at about the 10% level. Only for VAS channel 8 is the differences greater than a factor of two, and for VAS channel 12 the difference is about 50% of the larger value. In these larger difference cases the structure-estimated noise levels are greater than the repeat-view variabilities, due to either the inability to remove all of the spatial gradient information from the structure analysis, or due to additional components other than random noise in the data. One of these additional non-random noise components may be due to differences between the two (one upper and one lower) sensors used to simultaneously take measurements on two different scan lines. Secondly, there may be variability between the measurements on different scan lines due to changes in the calibration applied to each

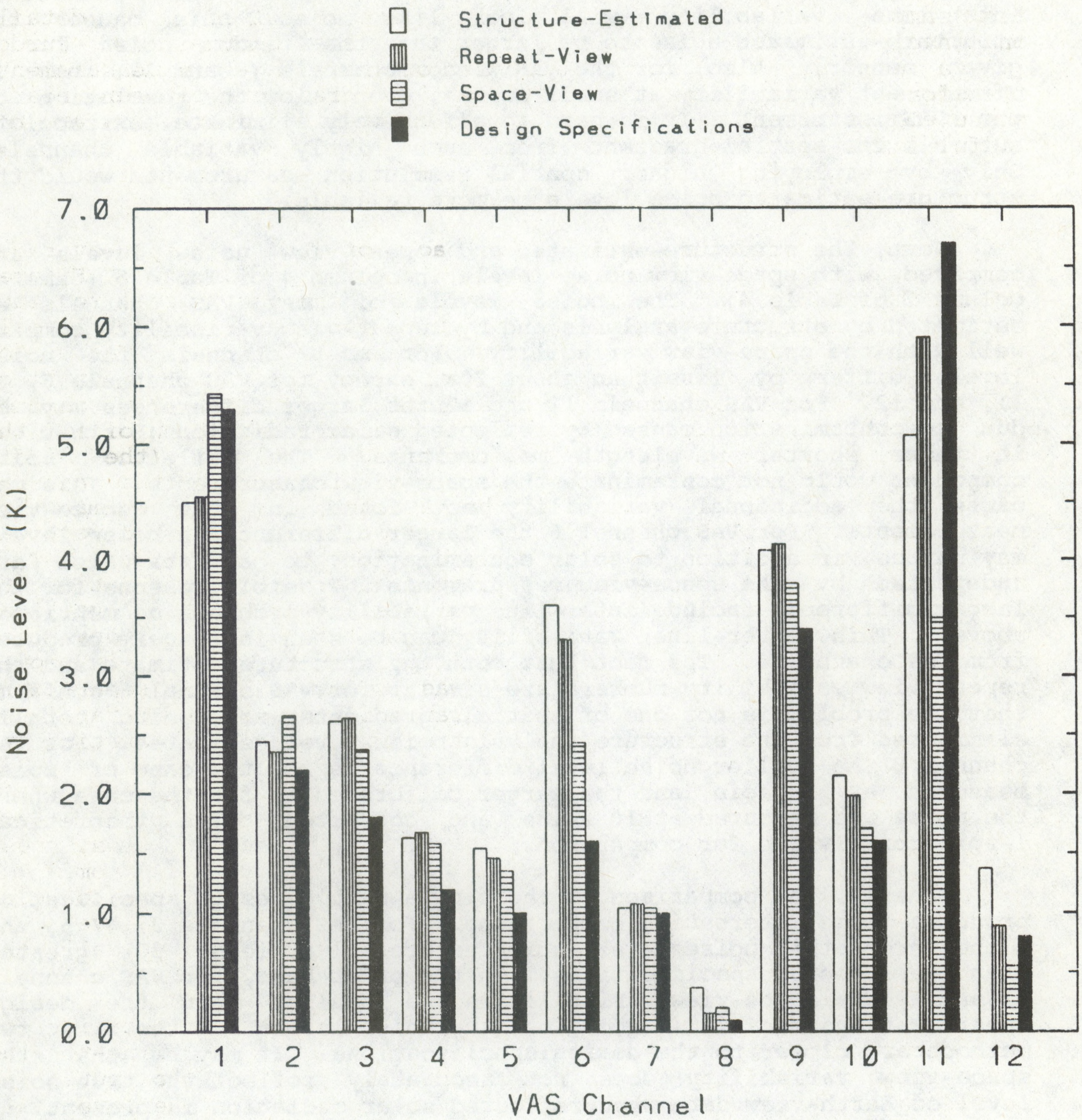

Figure 7: Comparison of single-sample (1-spin) noise levels from the three different analysis methods to the pre-launch design specifications for each of the 12 VAS channels. The numbers are the same as in Table 5. For each VAS channel vertical bars with different shading are used for each analysis method.

scan line of data. Third, there may be non-negligible line start timing errors which cause mis-alignments between the individual measurements from different spins (Menzel, 1980). Again, this is a non-random error component affecting the Earth-view measurements, not the space-view data. In any of these situations this additional inter-line variability will look like noise, this causes the structure-estimated noise to be larger than the random noise for a given sensor. Also, for the VAS window channels (8 and 12) there is often great variability at small scales, even below the resolution of the VAS instrument. It is hard to effectively eliminate (extrapolate out) all the spatial gradient from such highly variable channels. Only by employing higher spatial resolution measurements would the structure-estimated noise levels be more reliable.

Next, the structure-estimated and repeat-view noise levels are compared with space-view noise levels in column 4 of Table 5 (same as column 7 of Table 4). The noise levels of most VAS channels as estimated by structure analysis and by repeat-view variability compare well with the space-view variability. For most channels the noise levels differ by less than about 20%, except for VAS channels 6, 8, 11, and 12. For VAS channels 11 and 12 the larger differences may be due to contamination caused by reflected solar radiation (Earth-view) in these shorter wavelength measurements. The reflected solar component would not contaminate the space-view measurements. This may cause the additional variability not found in the space-view measurements. For VAS channel 6 the larger difference in noise levels may be due, in addition to solar contamination, to bad data which are undetected by the space-view measurements. Possible reasons for the larger difference include inter-line variability problems as mentioned above. This inter-line variability can be seen in imagery produced from VAS channel 6. The fact that both the structure-estimate and the repeat-view variability numbers are similar for VAS channel 6 confirms that the problem is not one of spatial gradients not being totally eliminated from the structure analysis noise level estimates. For VAS channel 8 the smaller noise level difference is for the case of noise measured at 1 spin, and the larger difference is for the case where the noise was measured at 10 spins and converted to a theoretical 1-spin noise value for comparison.

Finally, the comparison to the single-sample design specification produces some interesting comparisons. For VAS channels 3, 4, 5, and 6 the three other noise level estimates are all at least 30% greater than the design specifications. On the other hand, for VAS channels 11 and 12 the space-view variabilities are smaller than the design specifications. This is good, but the noise levels for the first two methods are closer to the design specifications. It may be that the space-view variability does not accurately reflect the true noise level of Earth-view data when reflected solar radiation is present.

6.1 Comparisons With Multiple Spins

Tables 6, 7, and 8 give comparisons similar to those in Table 5 between the noise levels determined by the three analysis methods, but without the inclusion of the design specifications. Table 6 is for 2 spins, Table 7 for 5 spins, and Table 8 for 10 spins. In each comparison column 2 is the structure-estimated noise level, column 3 is the repeat-view variability (when available), and the last column is the space-view variability. As explained above, the repeat-view variability is not available for more than 5 spins (Table 8).

Table 6

2-spin Noise Level Comparison

VAS Channel	Structure Estimate (K)	Repeat-view* Variability (K)	Space-view Variability (K)
1	2.99	3.01	3.84
2	1.67	1.58	1.88
3	1.88	1.78	1.67
4	1.31	1.10	1.12
5	1.06	0.98	0.96
6	2.68	2.19	1.70
7	0.74	0.73	0.73
8(1-spin)	0.35	0.11	0.085
8(10-spin)	0.35	0.11	0.15
9	3.08	2.78	2.68
10	1.45	1.31	1.24
11	4.06	3.93	2.48
12	1.15	0.59	0.39

* from Table 3, column 3

Table 7

5-spin Noise Level Comparison

VAS Channel	Structure Estimate (K)	Repeat-view* Variability (K)	Space-view Variability (K)
1	2.09	1.48	2.42
2	1.07	0.77	1.20
3	1.21	0.91	1.06
4	0.93	0.58	0.71
5	0.81	0.51	0.61
6	1.82	1.12	1.13
7	0.53	0.38	0.46
8(1-spin)	0.35	0.053	0.054
8(10-spin)	0.35	0.053	0.095
9	1.95	1.36	1.72
10	1.01	0.66	0.77
11	2.84	1.97	1.56
12	0.94	0.27	0.25

* from Table 3, column 4

Table 8

10-spin Noise Level Comparison

VAS Channel	Structure Estimate (K)	Space-view* Variability (K)
1	1.58	1.72
2	0.88	0.84
3	0.99	0.75
4	0.66	0.50
5	0.68	0.43
6	1.35	0.78
7	0.41	0.33
8(1-spin)	0.35	0.038
8(10-spin)	0.35	0.064
9	1.53	1.20
10	0.66	0.54
11	2.06	1.01
12	0.92	0.18

* from Table 4, column 5

In the 2-spin and 5-spin cases the structure-estimated noise levels are over twice as large as the repeat-view variability for VAS channels 8 and 12. The structure-estimated noise levels for these window and near-window channels are exaggerated because they do not have all of the the spatial gradient information removed. Also in the 2-spin comparison, the repeat-view variabilities are much greater than the space-view variabilities for VAS channels 6, 11, and 12. This discrepancy is in agreement with the single-sample comparisons in Table 5, showing that something is exaggerating the noise levels of Earth-view measurements which is not detected by the space-view measurements. For 5-spins the repeat-view and space-view variabilities are much closer than for 1 or 2 spins. Finally in the 10-spin comparison the structure-estimated noise levels for VAS channels 6, 8, 11, and 12 are over twice as large as the space-view variabilities. For VAS channels 8 and 12 the differences are especially large. In both of these channels the structure-estimated noise levels did not decrease as fast as theoretically expected with increasing number of spins. That was noticed by comparing the structure-estimated noise levels as a function of number of spins to the expected theoretical decrease with increasing number of samples (in Section 3.2). The noise levels for both VAS channels 8 and 12 did not decrease as rapidly as the theoretical curves in Figure 5. However, the theoretical decrease in noise is only true for totally random noise, not if other non-random factors influence the measured noise. For larger number of spins (Tables 7 and 8) the differences between the noise levels are more pronounced. For these VAS channels the repeat-view variabilities are better indications of the noise levels than the structure estimates. Also, the space-view variabilities were measured at 10 spins (and computed for smaller numbers of spins, except for VAS channel 8) making them more reliable in this comparison.

7.0 EFFECT OF NOISE ON TEMPERATURE AND DEW POINT RETRIEVALS

The effect of spin budget on retrieved temperature and dew point temperatures is shown in Figures 8a through 8d. Shown on each plot are three VAS retrievals. One retrieval (the center temperature and dew point temperature traces) is produced from a set of climatological-mean radiances. The absolute values are not of great importance, rather how the profiles change with added noise. The other two retrievals are produced from the same VAS channel measurements either increased or decreased by one standard deviation in noise. Whether the radiance in a particular VAS channel was increased or decreased by noise was determined by a random number generator. The sign of the change due to noise was determined randomly to avoid over-estimation or under-estimation of the effect of noise on retrieved soundings. The range in retrieved temperatures and dew point temperatures can easily be exaggerated if the signs of the noise levels are correlated for similar channels. Results for only one random number sequence are shown. Other random number scenarios are also possible. The important effect to notice, however, is how increasing the number of spins decreases the range of possible retrievals. Figure 8a shows the variation in retrievals for the case of only 1 spin per channel (the largest noise levels). Figure 8b shows the range in retrievals for 2 spins, Figure 8c shows the range in retrievals for 5 spins, and Figure 8d shows the results for 10 spins.

The decrease in variability of the retrievals by increasing from 1 to 2 spins is significant, showing how slight changes in spin budget can dramatically affect the resulting retrieval variability. The change per spin from 2 to 5 spins or from 5 to 10 spins is not as great as the change from 1 to 2 spins, indicating that collecting a limited number of spins is more important than collecting numerous spins for the same channels. This agrees with the most rapid decreases in noise levels at small number of spins, as was seen in Figure 5. However, it is best to use Table 2 as a guide to determine the optimal number of spins for each VAS channel, rather than this composite indication.

8.0 OPTIONAL SPATIAL AVERAGING

The noise levels given above are single-FOV values. By spatial averaging of several FOVs, noise levels can be further reduced to the requirements for producing thermodynamic soundings. However, arbitrary spatial averaging can destroy mesoscale gradient information in the VAS measurements. To avoid this, there is a way to reduce noise without destroying gradient information, by grouping (averaging) together only those measurements which are similar to within instrumental noise levels. For examples of this technique applied to VAS data, see Hillger and Purdom (1990) and Hillger, et al (1990).

9.0 SUMMARY AND CONCLUSIONS

Special VAS data were collected during December 1989 to determine the noise levels of VAS channels as a function of the number of spins (samples) per channel. Three noise level analysis methods were employed. Structure function analysis of adjacent FOVs was used to statistically determine the noise levels of the VAS channels. Results

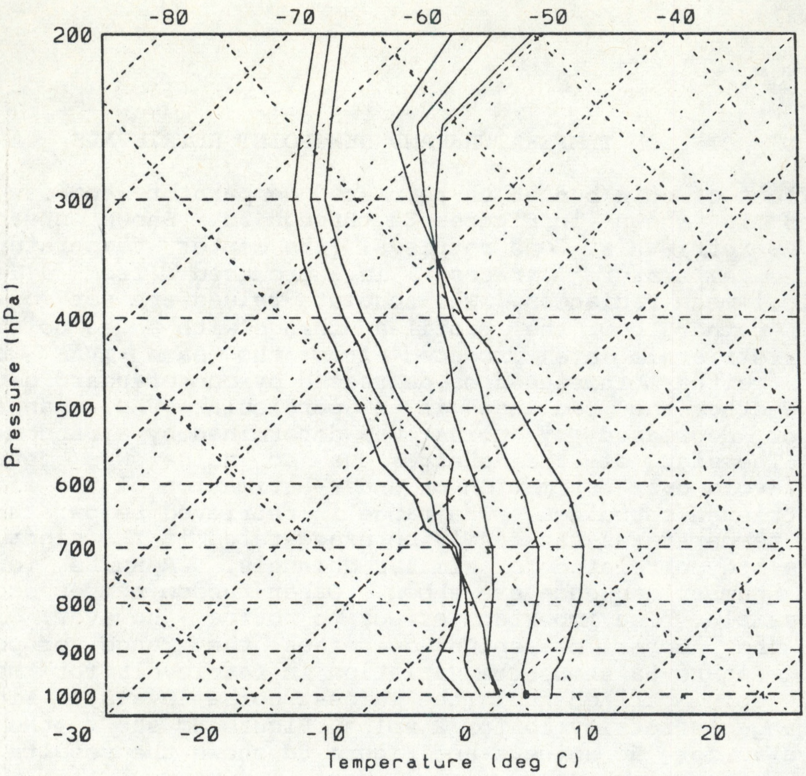

Figure 8a: Examples of the effect of noise levels on the range of retrieved temperatures and dew point temperatures. Three lines are soundings retrieved from a set of climatological-mean VAS radiances and the mean values in all VAS channels either increased or decreased randomly by one standard deviation in noise for one spin per channel.

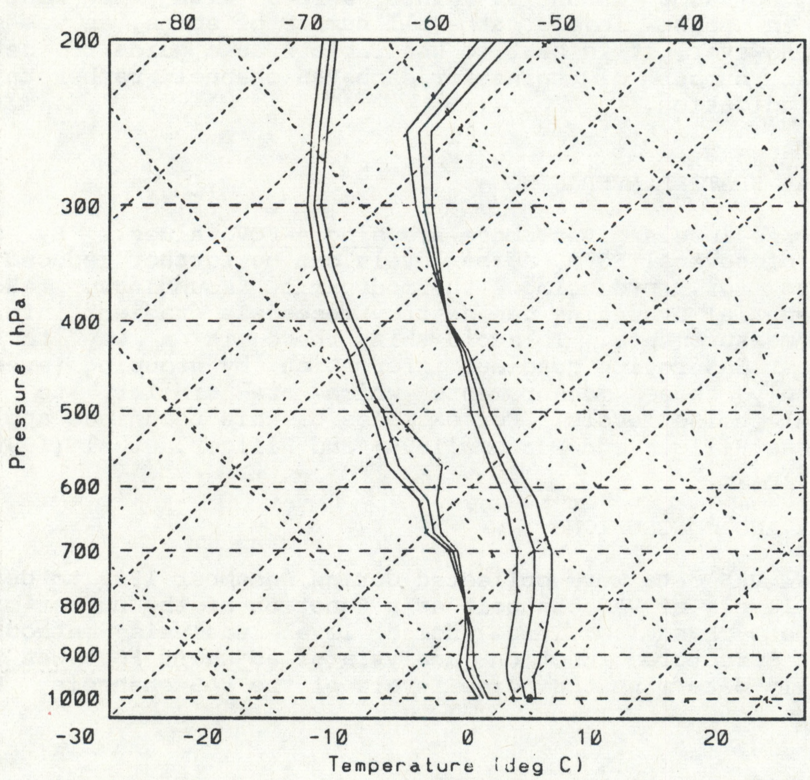

Figure 8b: Same as Figure 8a, but for 2 spins per channel.

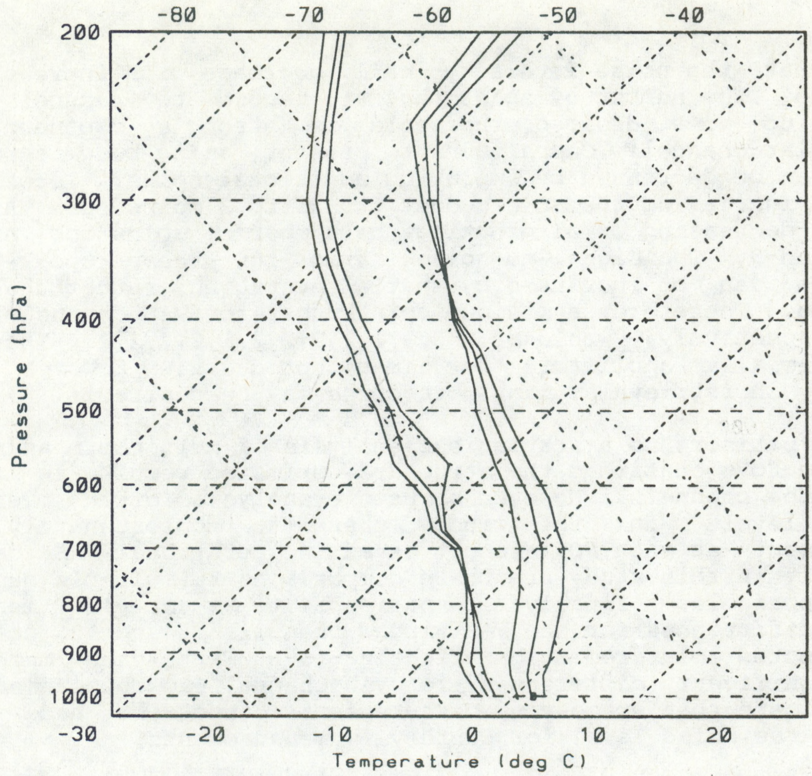

Figure 8c: Same as Figure 8a, but for 5 spins per channel.

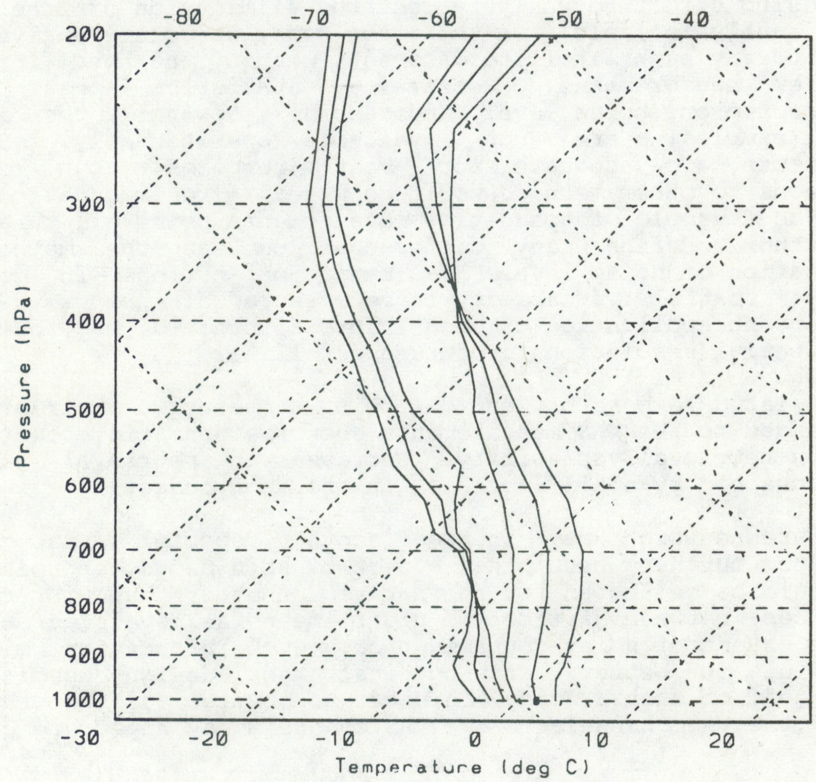

Figure 8d: Same as Figure 8a, but for 10 spins per channel.

show that the noise levels typically decrease with increasing number of spins. The number of spins that are needed to reduce the noise level to some desired threshold is strongly dependent on the particular channel. Comparisons to present spin budgets show that noise can be decreased by employing additional spins. Recommendations include increasing the spin budget from 1 to 2 spins for VAS channel 12, and decreasing or eliminating the number of spins for VAS channels 1, 2, and 3. The signal-to-noise ratio for these upper-level VAS channels can be increased by spatial averaging, rather than multiple sampling. Therefore, a minimum spin budget for VAS channels 1 through 12, respectively, would be: 0,1,1,2,2,2,2,1,2,2,2,2. These numbers are especially applicable for image products. However for more accuracy in retrievals, many more spins may be desirable.

Comparisons to a statistical analysis of multiple measurements at the same FOVs confirmed the structure-estimated results in many of the non-window channels. However structure analysis often overestimates noise levels in the window channels. Unfortunately multiple measurements at each FOV are not saved in operational VAS data sets. So, only in this study are these comparisons to multiple sample noise levels possible. Finally, comparisons to space-view measurements showed differences for the VAS window channels (8 and 12) possibly due to reflected solar radiation affecting the Earth-view measurements, and significant differences for VAS channel 6. These discrepancies may indicate that space-view measurements cannot be used alone to predict the noise level for Earth-view measurements.

Of the three methods used to determine noise levels, each has its advantages and disadvantages. Noise levels computed using structure analysis can be exaggerated for channels with spatial variability below the resolution of the satellite instrument. To determine noise levels using structure analysis requires elimination of the gradient in the analysis field. On the other hand, structure analysis can be applied to any such satellite data set, without the need for special space-view measurements. Repeat-view statistics appear to be the least error prone noise level indicators. However, the individual spins (samples) are not available operationally. Space-view measurements are adequate for most purposes, but occasional comparisons to other methods would be wise. A recommendation would be to analyze a sample of space-view measurements using all three methods to further define any differences between the methods. The determination of noise levels has many implications in conjunction with the spatial variability to be measured at various wavelengths. One important application of such information could be to determine sensor spatial resolution for future satellites.

Simulated temperature and dew point temperature retrievals with noise added to the VAS measurements show the dramatic effect of noise levels on retrieval variability. Decreases in retrieval variability can be obtained by small increases in the spin budget.

Future research may include another special data collection period to further test the effect of spin budget on noise levels. Data should be collected for another season other than winter. Also, differences between daytime and nighttime noise levels can be used to tell the extent of solar contamination. Such information might also be useful in better defining instrument design specifications. Another goal of such a study would be to better define the signal level of the VAS channels. Some VAS channels may appear to have large signal-to-noise ratios in large temperature gradient situations, while weak, although significant, temperature gradients may not be easily detected. Another goal would be to statistically analyze some space-view measurements, or some measurements over the ocean, using the same two techniques used for the Earth-view data. It is also possible to separately determine the noise levels of the upper and lower sensors for each channel by analyzing the measurements from each detector independently, which was not done in this study.

This study of noise levels has implications for GOES-Next, which will include many channels similar to those on the present GOES. GOES-Next will not use multiple samples of the same FOVs to decrease noise levels, but the dwell time may be increased to decrease noise levels. The decrease in noise level with increasing dwell time should be tested using some of the first data collected from GOES-Next.

ACKNOWLEDGEMENTS

The authors thank W. P. Menzel of NESDIS/CIMSS for arranging the special VAS data collection used in this study and T. J. Schmit for the space-view noise level analysis. Both Dr. Menzel and Mr. Schmit provided valuable feedback on the results presented in this report. Reviews of the manuscript were also provided by Dr. G. G. Campbell and Dr. S. B. Smith. This work was supported by NOAA Grant NA85RAH05045.

REFERENCES

Chesters,D., and W.D.Robinson, 1983: Performance appraisal of VAS radiometry for GOES-4, -5 and -6. NASA/GSFC, Technical Memorandum 85125, 55-p.

Chesters,D., W.P.Menzel, H.E.Montgomery, and W.D.Robinson, 1985: VAS instrument performance appraisal. [in VAS Demonstration: (VISSR Atmospheric Sounder) Description and Final Report. NASA Reference Publication 1151], NASA-GSFC, 17-33.

Gabriel,P.J., and J.F.W.Purdom, 1990a: Deconvolution of GOES infrared data. Fifth Conference on Satellite Meteorology and Oceanography, AMS, 3-7 September, London, UK, 181-184.

Gabriel,P.J., and J.F.W.Purdom, 1990b: Deconvolution of GOES infrared data. CIRA Newsletter, 5, Spring, 1-8.

Gandin,L.S., 1963: Objective Analysis of Meterological Fields. Translated from Russian, Israel Program for Scientific Translation, Jerusalem, 242-p. [NTIS: TT-65-50007]

Gomis,D., and S.Alonso, 1988: Structure function responses in a limited area. Mon. Wea. Rev., 116, 2254-2264.

Hayden,C.H., 1988: GOES-VAS simultaneous temperature-moisture retrieval algorithm. J. Appl. Meteor., 27, 705-733.

Hillger,D.W., and J.F.W.Purdom, 1990: Clustering of satellite sounding radiances to enhance mesoscale meteorological retrievals. J. Appl. Meteor., 29, 1344-1351.

Hillger,D.W., J.S.Snook, and J.F.W.Purdom, 1990: A case study analysis of clustering applied to VAS measurements. Fifth Conference on Satellite Meteorology and Oceanography, AMS, 3-7 September, London, UK, 354-359.

Hillger,D.W., and T.H.Vonder Haar, 1979: An analysis of satellite infrared soundings at the mesoscale using statistical structure and correlation functions. J. Atmos. Sci., 36, 287-305.

Hillger,D.W., and T.H.Vonder Haar, 1988: Estimating noise levels of remotely-sensed measurements from satellites using spatial structure analysis. J. Atmos. Ocean. Tech., 5, 206-214.

Menzel,W.P., 1980: Pre-launch study report of VAS-D performance, Cooperative Institute for Meterological Satellite Studies, NASA Contract Report NAS5-21965, 65-p.

Menzel,W.P., and T.J.Schmit, 1990: Personal communication.

Wald,L., 1989: Some examples of the use of structure functions in the analysis of satellite images of the ocean. Photogrammetric Engineering and Remote Sensing, 55, 1487-1490.

*U.S.G.P.O:1991-281-559:40005

(continued from inside cover)

NESDIS 23 The Use of TOMS Data in Evaluating and Improving the Total Ozone from TOVS Measurements. James H. Lienesch and Prabhat K.K. Pandey, July 1985. (PB86 108412/AS)

NESDIS 24 Satellite-Derived Moisture Profiles. Andrew Timchalk, April 1986. (PB86 232923/AS)

NESDIS 26 Monthly and Seasonal Mean Outgoing Longwave Radiation and Anomalies. Arnold Gruber, Marylin Varnadore, Phillip A. Arkin, and Jay S. Winston, October 1987. (PB87160545/AS)

NESDIS 27 Estimation of Broadband Planetary Albedo from Operational Narrowband Satellite Measurements. James Wydick, April 1987. (PB88-107644/AS)

NESDIS 28 The AVHRR/HIRS Operational Method for Satellite Based Sea Surface Temperature Determination. Charles Walton, March 1987. (PB88-107594/AS)

NESDIS 29 The Complementary Roles of Microwave and Infrared Instruments in Atmospheric Sounding. Larry McMillin, February 1987. (PB87 184917/AS)

NESDIS 30 Planning for Future Generational Sensors and Other Priorities. James C. Fischer, June 1987. (PB87 220802/AS)

NESDIS 31 Data Processing Algorithms for Inferring Stratospheric Gas Concentrations from Balloon-Based Solar Occultation Data. I-Lok Chang (American University) and Michael P. Weinreb, April 1987. (PB87 196424)

NESDIS 32 Precipitation Detection with Satellite Microwave Data. Yang Chenggang and Andrew Timchalk, June 1988. (PB88-240239)

NESDIS 33 An Introduction to the GOES I-M Imager and Sounder Instruments and the GVAR Retransmission Format. Raymond J. Komajda (Mitre Corp) and Keith McKenzie, October 1987. (PB88-132709)

NESDIS 34 Balloon-Based Infrared Solar Occultation Measurements of Stratospheric O3, H2O, HNo3, and CF2C12. Michael P. Weinreb and I-Lok Chang (American University), September 1987. (PB88-132725)

NESDIS 35 Passive Microwave Observing From Environmental Satellites, A Status Report Based on NOAA's June 1-4, 1987, Conference in Williamsburg, Virginia. James C. Fischer, November 1987. (PB88-208236)

NESDIS 36 Pre-Launch Calibration of Channels 1 and 2 of the Advanced Very High Resolution Radiometer. C.R. Nagaraja Rao, October 1987. (PB88-157169 A/S)

NESDIS 39 General Determination of Earth Surface Type and Cloud Amount Using Multispectral AVHRR Data. Irwin Ruff and Arnold Gruber, February 1988. (PB88-199195/AS)

NESDIS 40 The GOES I-M System Functional Description. Carolyn Bradley (Mitre Corp), November 1988.

NESDIS 41 Report of the Earth Radiation Budget Requirements Review - 1987 Rosslyn, Virginia, 30 March - 3 April 1987. L.L. Stowe (Editor), June 1988.

NESDIS 42 Simulation Studies of Improved Sounding Systems. H. Yates, D. Wark, H. Aumann, N. Evans, N. Phillips, J. Sussking, L. McMillin, A. Goldman, M. Chahine, and L. Crone, February 1989.

NESDIS 43 Adjustment of Microwave Spectral Radiances of the Earth to a Fixed Angle of Progagation. D. Q. Wark, December 1988. (PB89-162556/AS)

NESDIS 44 Educator's Guide for Building and Operating Environmental Satellite Receiving Stations. R. Joe Summers, Chambersburg Senior High, February 1989.

NESDIS 45 Final Report on the Modulation and EMC Considerations for the HRPT Transmission System in the Post NOAA-M Polar Orbiting Satellite ERA. James C. Fischer (Editor), June 1989. (PB89-223812/AS)

NESDIS 46 MECCA Program Documentation. Kurt W. Hess, September 1989.

NESDIS 47 A General Method of Using Prior Information in a Simultaneous Equation System. Lawrence J. Crone, David S Crosby, and Larry M. McMillin, October 1989.

NESDIS 48 Reserved

NESDIS 49 Implementation of Reflectance Models in Operational AVHRR Radiation Budget Processing. V. Ray Taylor, February 1990.

NESDIS 50 A Comparison of ERBE and AVHRR Longwave Flux Estimates. A. Gruber, R. Ellingson, P. Ardanuy, M. Weiss, S.K. Yang, (Contributor: S.N. Oh).

NESDIS 51 The Impact of NOAA Satellite Soundings on the Numerical Analysis and Forecast System of the People's Republic of China. A. Gruber and W. Zonghao, May 1990.

NESDIS 52 Reserved

NESDIS 53 NOAA-9 Solar Backscatter Ultraviolet (SBUV/2) Instrument and Derived Ozone Data: A Status Report Based on a Review on January 29, 1990. Walter G. Planet, June 1990.

NESDIS 54 Evaluation of Data Reduction and Compositing of the NOAA Global Vegetation Index Product: A Case Study.. K.P. Gallo and J.F. Brown, July 1990.

NESDIS 55 Report of the Workshop on Radiometric Calibration of Satellite Sensors of Reflected Solar Radiation, March 27-28, 1990, Camp Springs, Maryland. Peter Abel (Editor), July 1990.

NOAA SCIENTIFIC AND TECHNICAL PUBLICATIONS

The National Oceanic and Atmospheric Administration was established as part of the Department of Commerce on October 3, 1970. The mission responsibilities of NOAA are to assess the socioeconomic impact of natural and technological changes in the environment and to monitor and predict the state of the solid Earth, the oceans and their living resources, the atmosphere, and the space environment of the Earth.

The major components of NOAA regularly produce various types of scientific and technical information in the following kinds of publications:

PROFESSIONAL PAPERS—Important definitive research results, major techniques, and special investigations.

CONTRACT AND GRANT REPORTS—Reports prepared by contractors or grantees under NOAA sponsorship.

ATLAS—Presentation of analyzed data generally in the form of maps showing distribution of rainfall, chemical and physical conditions of oceans and atmosphere, distribution of fishes and marine mammals, ionospheric conditions, etc.

TECHNICAL SERVICE PUBLICATIONS—Reports containing data, observations, instructions, etc. A partial listing includes data serials; prediction and outlook periodicals; technical manuals, training papers, planning reports, and information serials; and miscellaneous technical publications.

TECHNICAL REPORTS—Journal quality with extensive details, mathematical developments, or data listings.

TECHNICAL MEMORANDUMS—Reports of preliminary, partial, or negative research or technology results, interim instructions, and the like.

U.S. DEPARTMENT OF COMMERCE
NATIONAL OCEANIC AND ATMOSPHERIC ADMINISTRATION
NATIONAL ENVIRONMENTAL SATELLITE, DATA, AND INFORMATION SERVICE
Washington, D.C. 20233